Universidade do Minho
Escola de Medicina

Violina Baranauskaite Barbosa

Characterization of Hippo signalling pathway in chick lung development

outubro de 2018

Violina Baranauskaite Barbosa **Characterization of Hippo signalling pathway in chick lung development**

UMinho | 2018

Universidade do Minho
Escola de Medicina

Violina Baranauskaite Barbosa

Characterization of Hippo signalling pathway in chick lung development

Caracterização da via de sinalização Hippo no desenvolvimento pulmonar da galinha

Dissertação de Mestrado
Mestrado em Ciências da Saúde

Trabalho efetuado sob a orientação da
Doutora Rute Carina Silva Moura

outubro de 2018

Acknowledgments

I would like to thank the institution, ICVS and Medical School, for the opportunity to join this outstanding Master program.

Importantly, I wish to express my gratitude to the project supervisor Professor Rute Moura, for enriching experience throughout this academic period. Also, for kindly accommodating me in her team and for her patience, dedication, tolerance, guidance, encouragement and intellectual stimulation.

Thank you for ICVS scientific community, course colleagues, laboratory I1.03 and the staff members for collaboration, also being patience, considerate and helpful.

Ultimately, I would like to mention my family, and friends (independent on geographical location), for their presence in good and bad moments, emotional support and faith. I share my accomplishments with you.

The work presented in this dissertation was performed at the Surgical Sciences Research Domain of the Life and Health Sciences Research Institute (ICVS), School of Medicine, University of Minho, Braga, Portugal (ICVS/3B's – PT Government Associate Laboratory, Braga/Guimarães, Portugal). The work was supported by FEDER funds, through the Competitiveness Factors Operational Programme (COMPETE), and by National funds, through the Foundation for Science and Technology (FCT), under the scope of the Project POCI-01-0145-FEDER-007038; and by the Project NORTE-01-0145-FEDER-000013, supported by the Northern Portugal Regional Operational Programme (NORTE 2020), under the Portugal 2020 Partnership Agreement, through the European Regional Development Fund (FEDER).

Abstract

HIPPO signalling pathway, and its effector YAP, have been recognized as important growth regulators during embryonic development, adult tissue regeneration, homeostasis, and tumorigenesis. YAP phosphorylation status impacts the transcription of HIPPO target genes responsible for conveying HIPPO response. Curiously, the inhibition of this pathway in the liver causes overgrowth, whereas in pancreas hypoplasia, therefore suggesting phenotypic differences depending on the organ system. Nevertheless, the information regarding pulmonary development remains limited. Therefore, this project aims to determine HIPPO's role during pulmonary branching and, for the first time, in the avian animal model.

All experiments were conducted in embryonic chick lungs during early branching stages. The spatial distribution of HIPPO signalling members was characterized by *in situ* hybridization. Moreover, *in vitro* lung explant culture was performed for 48 hours, and protein levels of phosphorylated-YAP (pYAP)/YAP were evaluated by Western blot at two time-points (0 and 48 hours). Additionally, lung explants were cultured with verteporfin (VP) (5, 7.5 and 10 μM), which prevents YAP-TEAD binding, resulting in supressed transcription of target genes (*ctgf*). Subsequently, explants were also subjected to *in situ* hybridization for *ctgf*, to confirm successful HIPPO modulation. In addition, explants were morphometrically analysed to determine the impact of Hippo modulation on lung growth. Finally, lung explants were evaluated for cytotoxicity by LDH assay.

In situ hybridization revealed that all HIPPO signalling members are present in the developing lung, throughout early stages of chick lung branching, except for *mst2* and *lats2*. The western blot analysis revealed similar expression levels of both YAP and pYAP in the three stages studied. After 48 hours in culture, YAP and pYAP protein levels were slightly decreased when compared to 0 hours, nonetheless, the pYAP/YAP ratio was maintained. Lung explants treated with 7.5 and 10 μM of VP displayed statistically significant overall reduction in lung size, when compared to controls. VP-treated lung explants displayed a decrease in *ctgf* expression, in a dose-dependent manner, thus confirming alteration in HIPPO signalling. Lastly, the LDH assay revealed no cellular toxicity in all verteporfin conditions.

This study demonstrates, for the first time, the presence of HIPPO signalling in early stages of avian pulmonary branching. Gene/protein expression profile and pathway modulation studies indicate that HIPPO is active and possibly involved in lung growth control.

Resumo

A via de sinalização HIPPO, e seu efetor YAP, têm um papel importante na regulação do crescimento durante o desenvolvimento embrionário, regeneração de tecidos no adulto, homeostasia e tumorigénese. O estado de fosforilação da proteína YAP tem impacto na transcrição de genes alvo específicos, responsáveis por transmitir a resposta da via. Curiosamente, a inibição da via HIPPO no fígado causa crescimento, enquanto no pâncreas induz hipoplasia, sugerindo diferenças fenotípicas dependendo do órgão. No entanto, a informação disponível sobre o desenvolvimento pulmonar é ainda limitada. Assim, este projeto como objetivo determinar o papel da via HIPPO durante a ramificação pulmonar e, pela primeira vez, no modelo de galinha.

Neste sentido, utilizaram-se pulmões embrionários de galinha nos estadios iniciais de ramificação. O padrão de expressão dos componentes da via HIPPO foi caracterizado por hibridização *in situ*. Paralelamente, realizaram-se cultura de explantes pulmonares *in vitro*, durante 48 horas, e os níveis proteicos de YAP e YAP fosforilado (pYAP) foram avaliados por Western blot às 0 e 48 horas. Mais ainda, os explantes pulmonares foram tratados com verteporfina (5, 7,5 e 10 μM) que impede a ligação de YAP-TEAD resultando na supressão da transcrição de genes alvo (*ctgf*). Subsequentemente, os explantes foram analisados por hibridação *in situ* para *ctgf*, para confirmar a modulação da via HIPPO. Os explantes foram também analisados morfometricamente para determinar o impacto da modulação desta via no crescimento pulmonar. Finalmente, os explantes pulmonares foram avaliados quanto à citotoxicidade pelo ensaio de LDH.

A hibridização *in situ* revelou que todos os componentes da via HIPPO estão presentes no pulmão em desenvolvimento, nos estadios iniciais da ramificação do pulmão de galinha, com exceção de *mst2* e *lats2*. Por outro lado, a análise de Western blot revelou níveis de expressão semelhantes de YAP e pYAP nos estadios estudados. Após 48 horas, os níveis de proteína YAP e pYAP diminuíram quando comparados a 0 horas, no entanto, a relação pYAP/YAP manteve-se constante. Os explantes de pulmão tratados com 7,5 e 10 μM de verteporfina (VP) apresentaram uma redução global, e estatisticamente significativa, no tamanho do pulmão, quando comparados com o controlo. Os explantes de pulmão tratados com verteporfina exibiram uma diminuição na expressão de *ctgf*, dependente da dose, confirmando assim a alteração na sinalização de HIPPO. Por fim, o ensaio de LDH não revelou toxicidade celular nas condições de verteporfina testadas.

Este estudo demonstra, pela primeira vez, a presença da via de sinalização de HIPPO nos estadios iniciais da ramificação pulmonar de galinha. O perfil de expressão bem como os estudos de modulação da via

sugerem que a via HIPPO está ativa e possivelmente envolvida no controlo do crescimento pulmonar, em galinha.

Table of Contents

Figure Index

Annex I

Table Index

Abbreviations and Acronyms

AKT - Protein kinase B

AMOT - Angiomotin

AMOTL – Angiomotin-like 1 protein 1

AMPK – AMP activated protein kinase

BCIP - 5-bromo-4-chloro-3'-indolyphosphate p-toluidine salt

BMP - Bone morphogenic protein

BSA - Bovine Serum Albumin

cAMP – Cyclic Adenosine monophosphate

cDNA - Complementary DNA

CHAPS - (3-((3-cholamidopropyl) dimethylammonio)-1-propanesulfonate)

CRB3 - Crumbs proteins 3

CTGF – Connective tissue growth factor

DIG – Digoxigenin

DMSO - Dimethyl sulfoxide

dpc – Days post coitum

E – Embryonic day

EDTA - Ethylenediaminetetraacetic acid

EGTA - Ethylene glycol-bis(β-aminoethyl ether)-N,N,N′,N′-tetraacetic acid

FGF - Fibroblast growth factor

G12/13 - G-protein receptors coupled with subunit α12/13

GAPDH – Glyceraldehyde 3-phosphate dehydrogenase

GGPP - Geranylgeranyl Pyrophosphate

GPCR – G-protein coupled receptors

GPER - G-protein coupled oestrogen receptors

Gq/11 - G-protein receptors coupled with subunit αq/11

Gs - G-protein coupled receptor with subunit αs

HEPES - 4-(2-hydroxyethyl)-1-piperazineethanesulfonic acid

HRP - Horseradish peroxidase

IPTG – Isopropyl β-D-1-thiogalactopyranoside

ISH – *In situ* hybridization

LB - Luria-Bertani broth

LDH - Lactate dehydrogenase

LPA - Lysophosphatidic acid

MABT - Maleic acid buffer containing Tween 20

mRNA - Messenger RNA

NADH - Nicotinamide adenine dinucleotide with hydrogen

NBT – Nitro-blue tetrazolium chloride

NF2 - Neurofibromatosis type 2

NTMT - Alkaline phosphatase buffer

OD – Optical density

P – postnatal day

PBS - Phosphate-buffered saline

PBT - Phosphate-buffered saline containing Tween 20

PCR - Polymerase chain reaction

PKA – Protein kinase A

pYAP – Phosphorylated YAP

RA – Retinoic acid

RNA - Ribonucleic acid

S1P - Sphingosine 1-phospahatase

SDS - Sodium dodecyl sulphate

SDS-PAGE - Sodium dodecyl sulphate polyacrylamide gel electrophoresis

SHH - Sonic hedgehog

SREBP - Sterol regulatory element-binding proteins

TAO 1 - Serine/threonine-protein kinase 1

TAZ - WW domain-containing transcription regulator protein 1 (WWTR1)

TBS-T - Tris-buffered saline containing Tween 20

TEAD - TEA domain transcription factors (TEAD1-4)

TGF-β – Transforming growth factor beta

VP – Verteporfin, trade name Visudyne®

WNT - Wingless-related integration site

X-Gal – 5-bromo-4-chloro-3-indolyl-β-D-galactopyranoside

YAP – Yes associated protein (non-phosphorylated)

1.INTRODUCTION

1.1. Hippo signalling pathway

The pioneering studies in fruit fly, *Drosophila melanogaster*, uncovered that deletion *warts* (*wts*) gene lead to abnormal growth of several organs (Justice et al. 1995; Xu et al. 1995). The following research further observed that mutants of *salvador* (*sav*), *hippo* (*hpo*) and *mob* (*mats*) displayed tissue overgrowth similarly to *wts* deletion (Kango-Singh 2002; Tapon et al. 2002; Harvey et al. 2003; Jia et al. 2003; Pantalacci et al. 2003; Lai et al. 2005). Eventually, these members were grouped and entitled as HIPPO signalling pathway, due to dramatic organ overgrowth, mimicking the appearance of a hippopotamus, upon *hpo* deletion. Ultimately, HIPPO main effector *yap* (*yorkie* in *Drosophila*) was discovered by screening the proteins that interact with WTS (Huang et al. 2005). HIPPO signalling comprises an evolutionarily conserved signalling transduction mechanism that controls gene expression and, consequently, numerous cellular events. In mammals, Hippo is composed of a cascade of kinases, MST1/2 and LATS1/2, and their co-factors SAV and MOB1A/1B. LATS1/2 kinase acts upon YAP and TAZ, which behave as transcriptional co-activators. Once in the nucleus, YAP-TAZ complex requires TEAD family of transcription factors to activate target gene expression. The corresponding homologues in Drosophila are as follows: *hpo*, *wts*, *sav*, *mob1a/b*, *yki* and *sd*.

Together, studies in vertebrate and mammalian models demonstrated that HIPPO exerts its effect through co-effectors YAP/TAZ. The effectors require DNA-binding partners, such as TEAD, for activating the transcription of target genes involved in proliferation, progenitor fate, and survival. Upon defective regulation of HIPPO core members, there is an impairment of different cellular events (Cao et al. 2008; Zhang et al. 2012). Nonetheless, HIPPO modulation displays phenotypic differences depending on the organ system. For instance, YAP activation in the liver causes excessive organ overgrowth (Camargo et al. 2007a). Whereas pancreatic-specific deletion of *mst1* and *mst2* with subsequent activation of YAP, result in decreased organ size (Gao et al. 2013; George et al. 2012a).

1.1.1. The activation of Hippo cascade/machinery

When the HIPPO pathway is activated, MST1/2 phosphorylates LATS1/2 at its C-terminal hydrophobic motif, hence triggering LATS1/2 auto phosphorylation. Additionally, MST1/2 phosphorylates MOB1 that contributes to the full activation of LATS1/2 kinase. Moreover, SAV1 protein is also phosphorylated by MST1/2 kinase; SAV1 acts as a binding partner of MST1/2, therefore resulting in efficient LATS1/2 phosphorylation by MST1/2 (Yu et al. 2015a; Scheel and Hofmann 2003a). On its turn, the LATS kinases

phosphorylate YAP/TAZ, causing their cytoplasm retention and degradation, hence inhibiting their effector function.

Conversely, upon deactivation of HIPPO signalling, MST1/2 no longer phosphorylates LATS1/2 kinase that, consequently, does not phosphorylate YAP/TAZ; the non-phosphorylated form of YAP/TAZ is translocated into the nucleus, where it complexes with TEAD transcription factors thus promoting the expression of specific target genes (Yu et al. 2015a; Moya and Halder 2016; Meng et al. 2016; Yu et al. 2015b). The HIPPO activity is summarised in the Figure 1.

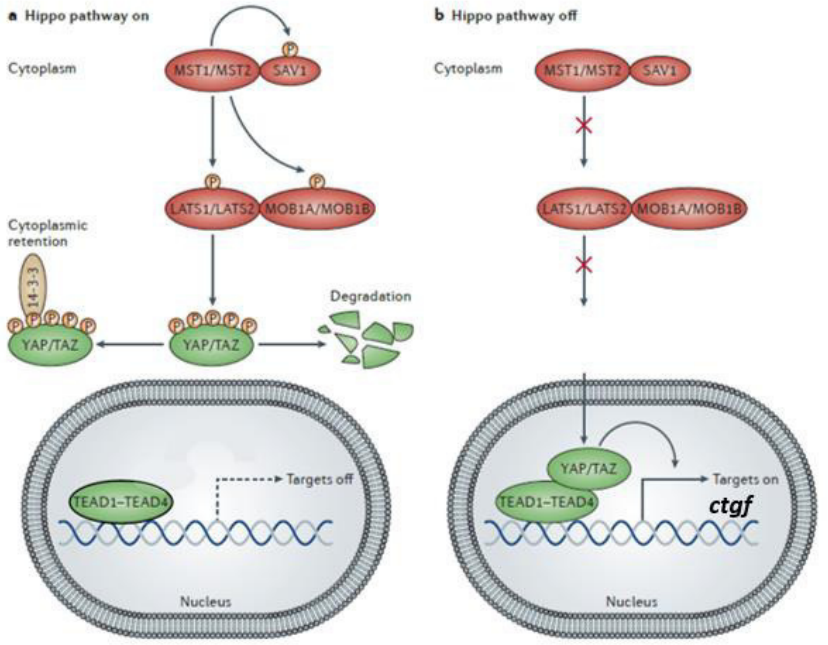

Figure 1. Schematic representation of Hippo signalling pathway. When Hippo pathway is on/active **(a**) the kinase cascade is activated resulting in YAP/TAZ phosphorylation, leading to cytoplasmic retention and degradation. Conversely, when the pathway is off/inactive **(b)** unphosphorylated YAP/TAZ translocate to the nucleus, hence binding to Tead transcription factors and activating transcription of target genes.

1.1.2. Hippo pathway modulation

Several HIPPO pathways modulators/inhibitors have been identified so far (Guo and Teng 2015; Woodard et al. 2017; Abylkassov and Xie 2016). The pathway may be modulated upstream through GPCR tumour suppressor NF2, TAO1 signalling, main inhibitory kinase MST/LATS.

1.1.2.1. Upstream Hippo modulation

HIPPO signalling can be modulated via G-protein coupled receptors (GPCRs). GPCRs belong to the largest family of plasma membrane proteins that convey extracellular soluble cues to the intracellular milieu. For

instance, lysophosphatidic acid (LPA) and sphingosine 1-phosphatase (S1P), present in the serum, exert their effect through G12/13 membrane receptors causing inhibition of LATS1/2 kinases and leading to dephosphorylation of YAP/TAZ at S127. In fact, LPA and S1P stimulate nuclear localization of YAP/TAZ in HEK293A and MCF10A cells in a dose-dependent manner. Conversely, cell lines cultured in serum-free medium presented elevated YAP/TAZ phosphorylation; moreover, YAP phospho-activation in S127 was showed to be independent to cell-cell contact. Additionally, LPA treatment supressed YAP binding to 14-3-3, but stimulated YAP-TEAD1 interaction resulting in increased expression of *ctgf* (YAP/TAZ target gene). On the other hand, ligand signalling via Gs (G-protein coupled receptor with subunit αs) activated LATS1/2 kinase, thus causing YAP/TAZ phosphorylation (Yu et al. 2012; Miller et al. 2012). Further examination using Rho GTPase, ROCK and F-actin inhibitors revealed blocked nuclear YAP localization mediated by S1P and LPA, suggesting that S1P and LPA regulate YAP via Rho GTPase and F-actin polymerization (Miller et al. 2012). Taken together, the ligand signal through G12/13 or Gq/11 (G-protein receptors coupled with subunit α12/13 and αq/11 respectively) activate YAP/TAZ, while Gs supress YAP/TAZ activity (Yu et al. 2012; Miller et al. 2012).

GPCRs are master regulators of other signalling pathways, as for instance, WNT signalling. Frizzled (FZD) belongs to the GPCR family and is involved in the regulation of non-canonical WNT (Anastas and Moon 2013). Recently, an alternative WNT-YAP/TAZ signalling axis has been reported comprising a WNT-FZD-G12/13-Rho-LATS1/2-YAP/TAZ-TEAD cascade that ultimately activates of YAP/TAZ-TEAD; this axis is independent of canonical WNT/βcatenin signalling. Nevertheless, the YAP/TAZ-TEAD binding promoted the expression of secreted WNT inhibitors thus antagonizing WNT/β-catenin signalling. This mechanism was necessary for differentiation in adipocytes (Park et al. 2015).

The β-adrenergic receptor is a G-protein-coupled receptor involved in many physiological responses. It has been shown that β-adrenergic receptor agonist dobutamine stimulates the cytoplasmic shift of YAP by phosphorylating S127 residue and supressing YAP-dependent TEAD transcriptional activity. Surprisingly, neither LAST1/2 nor AKT were involved in dobutamine mediated YAP phosphorylation. AKT was found to be active in U2OS cells when treated with dobutamine suggesting that YAP phosphorylation is induced via an unidentified kinase (Bao et al. 2011). However, further studies suggest otherwise, that dobutamine phospho-activates YAP through HIPPO pathway. According to Yu et al., cAMP signals via PKA, which requires Rho GTPases to activate LAST kinase, with subsequent YAP phosphorylation (Yu et al. 2013). Kim et al, had similar observations of cAMP/PKA mediate YAP phosphorylation through LATS

(Kim et al. 2013b). Additionally, cAMP sits downstream of Gs-coupled receptor (Yu et al. 2013), required for dobutamine stimulated YAP phospho-activation (Yu et al. 2012; Bao et al. 2011).

The tumour suppressor gene *nf2* (Neurofibromatin 2 in mammalian) or *merlin* (in *Drosophila*) is an important player in HIPPO signalling cascade activation. Studies in mammalian liver showed that inactivation of NF2 leads to hyperplasia of hepatocytes, hepatocellular carcinoma and bile duct hamartoma. This NF2-loss phenotype was reversed by YAP heterozygosity. Conversely, upon the loss of YAP, the livers showed defects in bile duct development and hepatocyte survival. These results suggest an antagonistic role of NF2 and YAP in liver homeostasis. Nonetheless, NF2 loss *in vivo* causes a reduction in LATS1/2 and YAP phosphorylation, which explains elevated proliferation in bile duct and hepatocytes. Altogether, it appears that NF2 functions upstream to regulate HIPPO core members (Zhang et al. 2010). Further investigation revealed that NF2/MERLIN regulates HIPPO without activating MST/HPO kinase in both mammals and Drosophila. Instead, NF2/MERLIN directly binds to LATS1/2 kinase at the plasma membrane, which is subsequently activated by MST-SAV complex (Yin et al. 2013).

It has been observed that suppression of TAO-1 (Serine/threonine-protein kinase) leads to organ overgrowth, a phenotype similar to mutations in HSW (HIPPO-SALVADOR-WART/LATS) pathway genes. The experiments in *Drosophila* suggest that TAO-1 directly phosphorylates HPO and promotes HSW pathway activation. This regulatory mechanism appears to be conserved in mammals. Moreover, genetic and biochemical analysis locate TAO-1 upstream of HPO (Boggiano et al. 2011).

1.1.2.2. Negative regulation loop

Studies suggest that YAP/TAZ can induce a negative feedback loop in two ways: by upregulating the expression of *last2* and *amotl2* (tight junction protein), which activates upstream negative regulator LATS1/2; or activating LATS inhibitory kinase through NF2 induction. Both activation loops require TEAD-mediated gene transcription (Dai et al. 2015; Moroishi et al. 2015; Zhao et al. 2008). Overall, this activation-initiated negative feedback loop suggests that once YAP/TAZ is nuclear, it will induce LATS1/2 phospho-activation (through NF2), which in turn phosphorylates YAP/TAZ, hence stabilizing their activity. This transient fluctuation between active and inactive YAP/TAZ provide the evidence of tight coordination of HIPPO pathway in maintaining the homeostasis.

1.1.2.3. Metabolic cues

Cellular energy stress, due to the inhibition of glucose metabolism and subsequent reduction of ATP levels, causes YAP phosphorylation, cytoplasmic retention and supressed transcriptional activity. AMPK (AMP-activated protein kinase), AMOTL1 (tight junction protein) and LATS1/2 are key regulators of YAP

activity. The energy stress activates AMPK, which directly phosphorylates AMOTL1 resulting in protein stability. Eventually, the accumulation of AMOTL1 leads to YAP inhibition by S127 phosphorylation (DeRan et al. 2014) and activation of LAT1/2 inhibitory kinase (Paramasivama et al. 2011). Moreover, AMOTL1 is involved in promoting YAP ubiquitination (Adler et al. 2013). In fact, the energy stress sensor AMPK directly phosphorylates YAP on S94 causing cytosolic retention which leads to supressed YAP-TEAD interaction. Moreover, this energy stress dependent YAP inhibition is exerted through LATS-dependent and -independent mechanism (Mo et al. 2015).

Recent studies suggest that the mevalonate pathway is necessary for YAP/TAZ transcriptional program. The mevalonate induced YAP/TAZ activity via production of GGPP (geranylgeranyl pyrophosphate) and through Rho GTPases. Curiously, this YAP/TAZ regulation bypasses inhibitory kinase LATS1/2 activation; also, Rho signalling can indirectly phosphorylate YAP/TAZ hence suggesting yet unknown YAP inhibitor kinase. Mevalonate/SREBP (membrane-bound transcription factors) pathway is involved in cell structure and signalling, nutrient levels and lipid metabolism (Brown and Goldstein 1997). Therefore, based on cellular needs, these metabolic signals impact YAP/TAZ activation (Sorrentino et al. 2014).

1.1.2.4. Mechanical cues

The cells are capable to adjust their cytoskeletal tension, morphology and proliferation rates according to the environmental cues. Moreover, changes in subcellular localization of YAP appear to coincide with this cell behaviour. Mechanical forces are regulators of YAP/TAZ in multicellular contexts, setting responsiveness to HIPPO and GPCR signalling. Mechanical stimuli such as cyclic or static stretch are associated with increased YAP transcriptional activity and nuclear localization. It was suggested that phosphorylated JNK kinase leads to reduced LATS activity and, consequently, elevated nuclear YAP levels (Codelia et al. 2014). Also, at high density, cells acquire small geometry leading to more cytoplasmic than nucleic YAP/TAZ (Bao et al. 2011). When cells experience low mechanical stresses, F-actin-capping proteins limit YAP/TAZ activity (Aragona et al. 2013). This YAP/TAZ mediated mechano-sensing is exerted through Rho GTPase signalling and actomyosin cytoskeleton tension, regardless of LAT1/2 kinase (Dupont et al. 2011). Moreover, mechanical stimuli, such as shear stress caused by the interstitial flow can induce differentiation. In these conditions, nuclear TAZ activation was observed, through Rho GTPase signalling, with upregulated transcriptional activity (Kim et al. 2013b).

1.1.2.5. Downstream Hippo modulation

The HIPPO pathway can be regulated downstream by interfering with the YAP/TAZ-TEAD complex, which directly impacts the transcription of target genes. For instance, VGLL4 (mammalian Vestigial-like protein)

targets YAP-TEAD interaction. Since VGLL4 does not have a DNA-binding domain, the transcriptional regulation is exerted by interacting with TEAD4. VGLL4 and YAP compete for the interaction with TEAD4 and, eventually, VGLL4 antagonises YAP by blocking its activity at the transcriptional level (Jiao et al. 2014). Chemical inhibitors, such as verteporfin (VP), mimic VGLL4 action since it directly interferes with YAP-TEAD association, hence hampering transcriptional activity (Liu-Chittenden et al. 2012). Additionally, VP functions by upregulating 14-3-3 protein and causing YAP cytoplasmic sequestration and degradation (Wang et al. 2016). Numerous studies recognized the efficacy of VP by direct YAP-TEAD targeting, especially in the cancer setting (Al-Moujahed et al. 2017; Liu-Chittenden et al. 2012; Dasari et al. 2017; Wei et al. 2017).

1.2. Hippo in early embryonic development

1.2.1. Cell polarity and position

Throughout preimplantation development, the fertilized egg undergoes numerous cleavage divisions, therefore producing increasing numbers of progressively smaller cells and, at the same time, maintaining the overall size of the embryo. During these divisions cells inherit a polarized state, generating two separate population of cells: polarized cells located on the outside of the embryo vs apolar cells located on the inside (Sasaki 2015; Cockburn and Rossant 2010a).

There are two models to explain the formation of two types of cells in early blastocyst stage (Sasaki 2015), and HIPPO has been related to one of them, the polarization model (Johnson and Ziomek 1981). It has been suggested that polar and apolar cells possess differences that will determine their inner/outer fate and differently regulate HIPPO signalling resulting in lineage-specific gene expression. In fact, high cytoplasmic levels of pYAP is a marker for inner cells (Anani et al. 2014), while nuclear YAP corresponds to outer cells (Nishioka et al. 2009). Moreover, HIPPO is also involved in cell-cell adhesion processes that are also required for positional information of the cell, through specific junction-associated proteins.

1.2.2. Specification of first lineages in blastocyst

Another important aspect of the preimplantation stage is the lineage specification. The differentiation of early blastocyst in two cell lineages trophectoderm (TE) and the inner cell mass (ICM) is regulated by transcription factors, such as *cdx2* and *oct3/4* respectively (Sasaki 2017; Cockburn and Rossant 2010b). TEA domain family transcription factors, specifically TEAD4, are upstream of *cdx2*, necessary for TE development (Nishioka et al. 2008). Moreover, nuclear YAP localization activated TEAD4 transcription factor in TE, therefore triggering *cdx2* transcription required for TE development. On the other hand, *tead4*

is suppressed in ICM via *lats* mediated YAP phosphorylation and maintaining YAP in the cytoplasm. Nonetheless, TAZ overexpression studies can increase *cdx2* expression and compensate for the absence of YAP during development. These findings confirm that both HIPPO effectors YAP and TAZ act together with TEAD to control *cdx2* expression during blastocyst formation (Nishioka et al. 2009).

Other studies report that *nf2* (homologue of merlin in *D. melanogaster*) is required for *lats1*/2- dependent YAP phosphorylation in the inside cells of pre-implantation embryos. This study demonstrated that maternal and zygotic *nf2* is present in pre-implantation embryos and only the ablation of both pools would dysregulate *yap*. Therefore, in these maternal-zygotic mutants, the inside cells fail to develop ICM lineage and acquire TE-like development, which results in preimplantation lethality. This further supports the essential role of HIPPO in the formation of functioning ICM, whereas in the absence of this pathway the cells will adopt TE fate (Cockburn et al. 2013).

1.3. Hippo in organ development

Recent studies indicate important roles of HIPPO signalling during embryonic development in different organ systems. For instance, inhibition of HIPPO signalling effectors YAP and TAZ result in aberrant coronary vasculature development, due to impaired epicardial epithelial-to-mesenchymal transition (EMT) and suppressed epicardial cell proliferation and differentiation into coronary endothelial cells. The study also reports that YAP and TAZ regulate epicardial cell proliferation, EMT and cellular fate by partial regulation of *tbx18* and *wt1* expression (Singh et al. 2016b). In addition, Gise et al. showed that *yap*1 activation in foetal and postnatal hearts stimulated cardiomyocyte proliferation. On the other hand, inactivation of *yap*1 in the embryonic heart resulted in lethal myocardial hypoplasia and supressed cardiomyocyte proliferation. Even though *yap*1 showed to be important for cardiomyocyte proliferation, it didn't contribute to their physiological hypertrophic growth (Gise et al. 2012b).

It has been described that *yap* isoform – *yap*1 is involved in skeletal development and postnatal growth by regulating chondrocyte maturation and differentiation. *yap*1 promotes early chondrocyte proliferation but inhibits their maturation both *in vitro* and *in vivo*. It has been shown that *yap*1 needs TEAD family transcription factors to be able to induce *sox6* expression thus promoting the proliferation of chondrocytes; however, it prevents the maturation by interacting with *runx2* and consequentially suppressing *col10a1* gene expression (Deng et al. 2016).

Neonatal mice developed severe renal hypodysplasia after conditional *nf2* deletion (in ureteric bud lineage - UB). Therefore, the impaired branching morphogenesis observed in nf2 mutants were due to

overactivation of YAP/TAZ and, consequently, upregulated proliferation. Further analysis in UB compartment (tip, tip adjacent, and trunk) revealed that cells with an elevated YAP activity display cell-autonomous defect and are unable to form UB tip domain. Overall, supressed YAP/TAZ activity was able to rescue NF2-deletion induced phenotype (Reginensi et al. 2016).

The study assessing the role of HIPPO pathway during embryonic stem (ES) cell pluripotency and lineage commitment, found that YAP phosphorylation levels were decreased in *mst-/-* ES cells, while NANOG (the pluripotency marker) levels were increased. Additionally, the *mst-/-* ES cells displayed defects in embryoid body (EB) formation and differentiation delay to cardiac progenitor cells (Li et al. 2013b).

1.4. Hippo in tissue regeneration

Despite the role throughout organogenesis, HIPPO pathway is involved in tissue regeneration and homeostasis. The liver is known for its regenerative capacity, after injury or partial hepatectomy. HIPPO signalling pathway was proposed to be an important regulator of liver regeneration and homeostasis. Once the adult liver encounters an injury, YAP becomes activated and causing proliferation of progenitor cells, but suppressing differentiation (Wang et al. 2017).

Studies in the mammalian adult liver show that activation of *yap*, by deletion of *mst1/2*, results in high proliferation culminating in an abnormal increase of organ size (Lu et al. 2010). Even though overexpression of *yap* causes liver overgrowth, this phenotype can be reversed by reducing *yap* activity (Camargo et al. 2007b; Dong et al. 2007). Meaning that modulation of *yap* could be potentially used for therapeutic purposes without having adverse effects (Moya and Halder 2016). Interestingly, in the pancreas, the *mst1/2* ablation resulted in hypoplasia instead of organ overgrowth (Gao et al. 2013; George et al. 2012b). Altogether, suggesting that, HIPPO signalling has organ exhibit specific effect.

Other study using rodents reported that cardiac-specific deletion of *yap* prevents neonatal heart regeneration; in contrast, the overexpression of constitutively active form of *yap* in adult hearts promotes cardiac regeneration by increasing the number of cardiomyocytes, reducing the scar size and improving cardiac function after MI. This regenerative capacity of HIPPO effector *yap* can be correlated to proliferation associated target genes. On the other hand, ablation of bot *yap* and *taz* in neonatal hearts resulted in lethal cardiomyopathy in a gene dosage-dependent manner. This study also reports redundant roles of *yap* and *taz* during cardiac development with the dominant role of *yap* over taz (Xin et al. 2013). More recently, Morikawa et al. (2015) identified direct YAP transcriptional target genes stimulating

cytoskeletal remodelling with cellular protrusions during heart regeneration. The polymerized F-actin stimulates YAP nuclear localization eventually contributing to cellular protrusions (Morikawa et al. 2015b).

In the bone, *yap* isoform – *yap*1 is involved in the bone reconstruction by inhibiting cartilaginous callus tissue formation and initiating fracture repair (Deng et al. 2016).

YAP is also necessary for the maintenance of adult mammalian stem cells. Self-renewal and differentiation are regulated by *yap* which, consequentially, leads to variations of epithelial architecture. Upon *yap* inactivation in adult airways, the basal stem cells are lost and undergo uncontrolled differentiation. However, overexpression of *yap* results in stem cell self-renewal, suppression of terminal differentiation and epithelial stratification, which can be reversed once *yap* expression is normalized. Also, the persistent overexpression of YAP in secretory cells, caused them to acquire a basal-like state, but YAP knockdown prevented these cells from dedifferentiation into stem cells (Zhao et al. 2014b).

1.5. Hippo signalling in tumorigenesis

During embryonic development, HIPPO pathway members have key roles in epithelial-to-mesenchymal transition (EMT), cellular proliferation and differentiation (Singh et al. 2016a; Gise et al. 2012a; Deng et al. 2016; Li et al. 2013a; Mahoney et al. 2014; Lange et al. 2015). HIPPO is also a key regulator in mediating organogenesis, tissue regeneration and homeostasis in foetal stages and postnatally (Wang et al. 2017; Morikawa et al. 2015a; Zhao et al. 2014a; Lange et al. 2015). Signalling pathways and transcription factors involved in embryonic development are also implicated in carcinogenesis and HIPPO pathway is not an exception.

Several studies have shown an upregulation of YAP/TAZ expression and/or nuclear sequestration in many cancers suggesting impaired HIPPO regulation. For instance, increased expression of TAZ coincides with invasive breast cancer. The TAZ upregulation in MCF10A normal breast cell line revealed a dramatic increase in migration and invasion properties. While the loss of function in MCF7 and Hs578T cell lines demonstrated opposite outcome, decreased migration, and invasion (Chan et al. 2008). Regarding YAP, enhanced and altered expression was detected in colon, lung ADC, and ovarian serous cystadenocarcinoma (OSC) (Steinhardt et al. 2008).

For instance, HIPPO pathway mutations associated with cancers are in tumour suppressor gene *nf2*. The Neurofibromatosis type 2 (NF2) is autosomal dominant disorder leading multiple benign tumours in the nervous systems like schwannomas and meningiomas (Xiao et al. 2003). Nonetheless, the *nf2*-deletion phenotype in the mammalian liver can be partially reversed by heterozygous deletion of YAP. This

suggests that HIPPO effector YAP could serve as a potential target against Neurofibromatosis type 2 (Zhang et al. 2010).

The impaired GPCR signalling mechanism is also associated with tumour formation. For instance, mutations in Gαq stimulate YAP nuclear accumulation through Trio-dependent-Rho GTPases resulting in actin polymerization and F-actin accumulation. This signalling circuit suggests YAP nuclear translocation without activating canonical HIPPO. Finally, YAP regulated transcription stimulated uveal melanoma cell growth and tumour formation (Feng et al. 2014). The YAP dephosphorylation and nuclear activation were observed in Gq/11 mutation. As in a previous study, nuclear YAP correlated with active transcription machinery, resulting in uveal melanoma tumorigenesis. Additionally, treatment with verteporfin supress tumour growth, hence implying that YAP is a potential therapeutic target for uveal melanoma (Yu et al. 2014). It is proposed, that Gs together with PKA belong to tumour suppressive circuit that limits YAP transcriptional activity and mediate stem cell fate. It has been described that Gs-PKA induced YAP inactivation via LATS inhibitory kinase and tumour suppressor protein NF2. Also, supressed Gs/PKA activity result in YAP nuclear activation leading to stem, cell expansion and basal-cell carcinoma (BCC), while the activation stem cell depletion. (Iglesias-Bartolome et al. 2015).

In breast cancer, oestrogen activates GPER (G-protein coupled estrogen receptors) through Gq/11 and Rho/ROCK signalling to activate YAP/TAZ oncoproteins. In this case, LATS1/2 kinase is inhibited and unable to phosphorylate YAP/TAZ. Surprisingly, the MST1/2 kinase is independent of YAP/TAZ dephosphorylation caused by GPER (Zhou et al. 2015).

1.6. Development of mammalian respiratory system

The development of the respiratory system is a continuous intricate process starting *in utero* and continuing postnatally. In the mammalian, epithelial tubules are organized into a tree-shaped structure (trachea and lung) where the air is cleaned, humidified and delivered to alveolar structures, for the gas exchange (Cardoso and Lü 2006; Ornitz and Yin 2012; Herriges and Morrisey 2014). The cellular specification, differentiation, and growth of the air-conducting system and gas exchange units depends on multiple signalling pathways and transcription factors (Swarr and Morrisey 2015).

In the primitive gut tube, the expression of particular transcription factors will define organ-specific sections, such as the respiratory tract, oesophagus, intestine, stomach, liver, pancreas and gallbladder. For instance, *nkx2.1 (ttf1)* expression in the ventral region of anterior foregut endoderm gives rise to lung/tracheal region (Figure 2A). Despite lung domain specification, *nkx2.1* is necessary for trachea

separation from oesophagus (Kimura et al. 1996; Minoo et al. 1999). The cooperation of WNT2 and WNT2B are crucial for specifying lung endoderm progenitors within the developing foregut. Furthermore, WNT2/2B expression does not impede the specification of other foregut-derived tissues (thyroid, oesophagus, liver, and pancreas). However, active canonical WNT/β-catenin signalling can reprogram posterior endoderm, giving rise to oesophagus and stomach into lung progenitor fate (Goss et al. 2009).

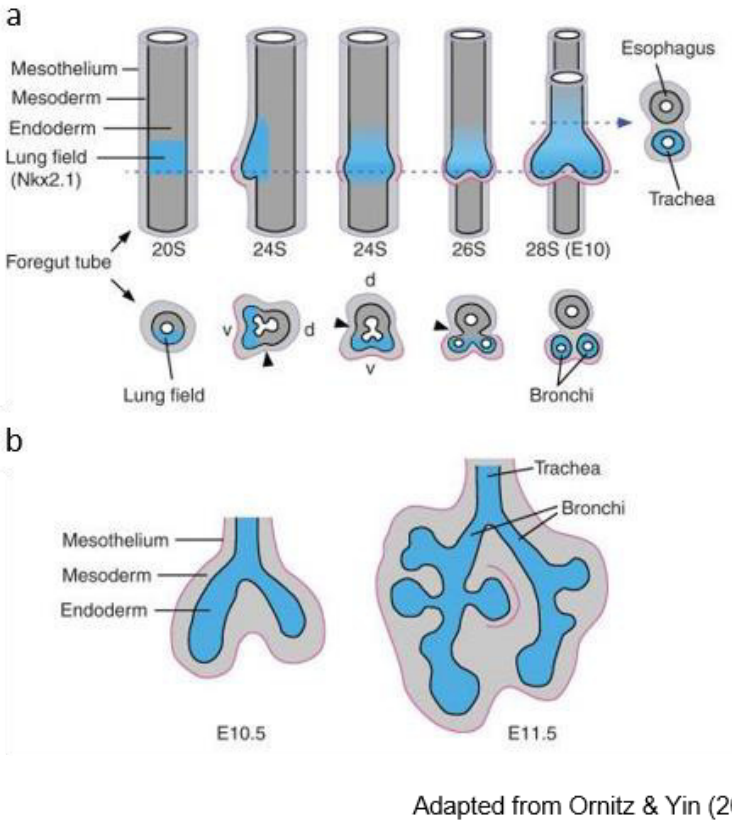

Adapted from Ornitz & Yin (2012)

Figure 2. Schematic representation of mammalian (mouse) lung development. (a) The lung specification in the ventral region of anterior foregut (blue), followed by tracheo-esophageal septation **(b)** The pseudoglandular stage (E10.5-E16.5) where coordinated branching morphogenesis occurs. E – embryonic day; S – somite.

Around E9.5, two endodermal lung buds start to emerge from ventral foregut to lateral direction and entering the surrounding mesenchyme. Eventually, these buds elongate and form primary lung buds (right and left). Meanwhile, the tracheal primordium initiates ventrally and separates from the dorsal gut tube resulting in the primitive oesophagus. Nonetheless, signalling molecules, such as BMP4, tune trachea and oesophagus morphogenesis. (Li et al. 2008).

Around E10.5, secondary buds begin to outgrow in different directions from the primary bronchial structure. Up until E16.5-E17.0, the pulmonary epithelium encounters further branching morphogenesis including repetitive series of bud outgrowth, elongation, bifurcation until the terminal branches are formed

(conducting airways and alveolar sacs) (Figure 2B) (Cardoso and Lü 2006). The lung branching is stereotypical, where the bronchial tree originates by (genetically regulated) three modes of branching, which occur in three different order. Domain branching refers to secondary branches emerging in rows at different positions around the circumference of the main bronchus and resembling rows of bristles on the bottle brush (Figure 3A). The secondary bronchi arise along the anterior-posterior axis (of the main bronchi) and give rise to tertiary bronchi, which bifurcate to create further branches. This repetitive process creates a series of tip divisions and occurring at the same plane – planar bifurcation (Figure 3B). During orthogonal bifurcation, the branches bifurcate at the tip and rotate at ≈ 90 °and forming a rosette (Figure 3C). From pseudoglandular stage onwards (E10.5-E16.5), these branching modes are repeated at different times and positions. The domain branching first gives rise to principal bronchi, a base for future lobes. During planar and orthogonal bifurcation, the branches both bifurcate and rotate, hence forming thin edges and filling the lobes (Metzger et al. 2008).

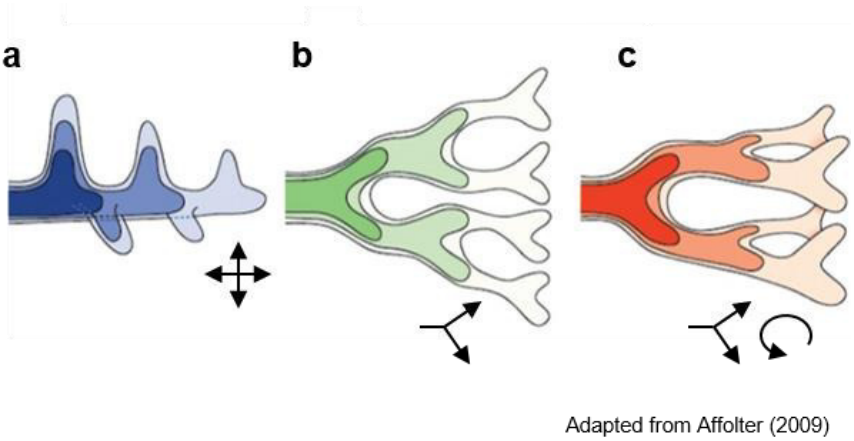

Figure 3. Schematic representation of branching modes in the mammalian. (a) domain branching **(b)** planar bifurcation **(c)** orthogonal bifurcation

During canalicular and saccular stage (E16.5-E17.5 and E18.5-P5, respectively) the terminal branches reorganize/develop into alveoli with subsequent maturation during alveolarization stage (P0-P14). Moreover, the lung mesoderm interacts with developing endoderm, hence stimulating branching and differentiation, while establishing different lung lineages (airway, vascular smooth muscle, pericytes).

Proper lung organogenesis relies on the interaction of multiple molecular pathways, such as fibroblast growth factor (FGF), bone morphogenic protein (BMP), wingless-related integration site (WNT), sonic hedgehog (SHH), Notch and retinoic acid (RA). Overall these signalling pathways are involved in primary (and subsequent) lung bud (bronchi) formation, also regulating proximal-distal patterning, epithelial-mesenchymal crosstalk, progenitor pool expansion, cellular proliferation and differentiation (Cardoso and

Lü 2006; Warburton et al. 2005; Lai 2004; Morrisey and Hogan 2010; Cardoso et al. 1995; Cardoso et al. 1996). Over the years, these molecular mechanisms were extensively studied, however additional information about already existing and newly emerging pathways are necessary to fully comprehend their role during lung organogenesis.

1.7. Development of avian respiratory system

The avian model (*Gallus gallus*) takes up a respectful position amongst other animal models. Despite well-addressed contributions in neuroscience, cancer biology, immunology, virology, cell biology, yet it has expanding potential as a cost-effective and efficient model for drug development. Chick embryos are an alternative for the mammalian, hence reducing the need for large groups of animals. Nevertheless, the avian model could serve as partial replacement to obtain perfused organs, tissue slices and cell culture which may substitute other laboratory animals (Vergara and Canto-Soler 2012; Bjørnstad et al. 2015). In fact, the avian model is used for studies of retinal (Vergara and Canto-Soler 2012) and cardiovascular development and cancer biology research (Kain et al. 2014).

Regarding the lung, although avian and mammalian respiratory system at the adult stages is distinct, they share morphological similarities in the early embryonic development. Particularly, during early branching morphogenesis. Additionally, common molecular pathways are associated with the early formation of both mammalian and chick respiratory system. At stage HH14, *nkx2.1* is detected in the ventral endoderm of the foregut in the oesophagus-respiratory region. At stage HH15, *tbx4* is found in the visceral mesoderm of the chick lung field. Moreover, *fgf10* expression in the chick lung primordium mesoderm is required for initiation of primary buds (Sakiyama et al. 2002). In the chick lung, once the two main bronchi are established, the secondary branches arise from the dorsal surface by monopodial branching, driven by apical constriction (Figure 4).

This conducting airway formation is anatomically similar to the domain branching of the mammalian lung (Figure 3a) (Tzou et al. 2016; Metzger et al. 2008; Kim et al. 2013a). Interestingly, the branching of mouse lung epithelium can be induced by chick mesenchyme. This suggest common mechanisms occurring in avian and mammalian pulmonary development (Sakiyama et al. 2000; Taderera 1967). Moreover, the spatial distribution of FGF (*fgf10, fgfr1-4 and spry2*), canonical SHH (*shh, ptch1, smo, gli1*, and *hhip*), WNT and Retinoic acid signalling members in embryonic chick lung are similar to their mammalian counterparts (Moura et al. 2011; Moura et al. 2014; Moura et al. 2016; Fernandes-Silva et al. 2017).

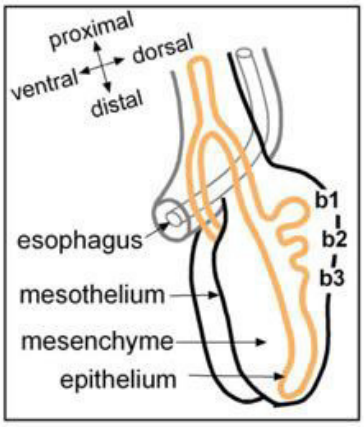

Adapted from Kim (2003)

Figure 4. Depiction of monopodial branching mode in chick lung

1.8. Hippo signalling in lung development

Multiple studies support the importance of HIPPO pathway during lung development. Even though bud initiation was not affected upon conditional removal of *yap* from developing lung epithelium, the bronchi arising from mutant lungs continued to expand and didn´t form into airways. Meaning that lung branching morphogenesis is impaired leading to the appearance of cyst-like structures. During lung organogenesis, epithelial progenitor cells balance signals between growth and differentiation. The HIPPO effector *yap* is involved in regulating this process. Nonetheless, *yap* phosphorylation and cytoplasmic localization is mandatory for epithelial cell differentiation into distinct phenotypes and formation of adult airways (Mahoney et al. 2014).

The *taz* knockout in rodents displayed changes in the kidney and lung, which mimicked polycystic kidney disease and pulmonary emphysema in humans. Mutant mice showed renal cyst formation with pelvic dilation, hydronephrosis and low survival rate after the birth. As these mice reach the adult stages, they displayed multicystic kidneys with urinary concentrating defects and polyuria. The lung demonstrated diffuse emphysematous changes upon *taz* deletion (Makita et al. 2008).

Additionally, manipulation of the upstream signals of YAP/TAZ, also show consequences during organogenesis. For instance, conditional deletion of *mst1/2* from epithelial progenitor in the foetal lung stimulated proliferation and inhibited epithelial cell differentiation, which resulted in lung hypercellularity, sacculation defects and perinatal lethality (Lange et al. 2015).

Another study focusing on the interaction between *mst1/2* and *yap* during lung growth in rodents report that epithelial loss of *mst1/2* can lead to neonatal lethality due to lung defects. Additionally, the pYAP to

total YAP ratio is reduced, which coincides with upregulation of YAP target genes. These findings are consistent with the negative role of *mst1/2* in regulating YAP. The neonatal lethality caused due to deletion of *mst1/2* can be rescued by removal of one allele of *yap* or one copy of both *yap* and *taz* (Lin et al. 2015).

Upon the lung injury, HIPPO effector *yap* is dynamically regulated and contributes to the regeneration of airway epithelium. The deletion of *mst1/2* in the adult lung and overexpression of *yap* in primary human bronchial epithelial cells (HBEC's) resulted in suppressed differentiation of different epithelial cells and increased proliferation. Upon removal of *mst1/2*, inhibitory YAP phosphorylation in the cytoplasm was reduced and instead fostering YAP nuclear presence and transcriptional activation of target genes (Lange et al. 2015).

Szymaniak and his team have shown that transmembrane proteins CRUMBS3 (CRB3) mediated polarity is necessary for airway differentiation, which is achieved by regulating sub-cellular localization of YAP. In the apical cell junctions, CRB3 promotes YAP binding with LATS1/2, causing YAP phosphorylation and cellular differentiation. On the other hand, the absence of CRB3 in both adult mouse airway progenitors and developing lungs triggered uncontrolled nuclear YAP activity causing differentiation defects (Szymaniak et al. 2015).

2.AIMS

HIPPO signalling has a key role in multiple physiologic processes, such as regulation of organ size and tissue homeostasis in both embryonic and adult stages. Through its kinase cascade, and cross-talk with other molecular pathways, HIPPO controls cellular events such as proliferation, differentiation and apoptosis (Yu et al. 2015; Saito and Nagase 2015; Hong and Guan 2012). HIPPO signalling has organ-specific effects due to the complexity and multiple functions of this pathway. In this sense, we hypothesize that HIPPO signalling might be a regulator of chick embryonic lung development and interact with other molecular pathways. Therefore, the main purpose of this project is to describe HIPPO pathway and its role during early pulmonary development in chick.

Firstly, we characterized the spatial distribution of HIPPO signalling components (*mst1/2*, *lats1/2*, *yap*, *taz*, *tead1* and *tead4*) and downstream target (*ctgf*) by *in situ* hybridization, and pathway activity was measured by assessing phosphorylated-YAP (pYAP) and YAP protein levels by western blot, in early stages of chick lung development.

Subsequently, pathway modulation study was performed to assess HIPPO signalling role; for that purpose, *in vitro* lung explants were treated with a YAP-TEAD complex inhibitor (Verteporfin) and then assessed for morphometric and cellular parameters. Successful HIPPO pathway modulation was verified by *in situ* hybridization for *ctgf* (Hippo target gene). Eventually, possible toxic effect on lung explants, caused by verteporfin treatment, was assessed by LDH assay.

The proposed project aims to fulfil the following objectives:

- Characterize the expression pattern of HIPPO signalling pathway components and downstream targets, in early stages of chick lung development.
- Assess HIPPO signalling activity in the avian lung.
- Determine the role of HIPPO signalling in chick lung branching.

3.MATERIALS AND METHODS

3.1. Ethical Issues

The work presented in this thesis was performed in the avian model (*Gallus gallus*), at early developmental stages. The ethical approval for using this animal model is not required from review board institution or the ethical committee; this is in accordance with the Directive 2010/63/EU of the European Parliament and of the Council of 22 September 2010 on the protection of animals used for scientific purposes. The Portuguese Directive 113/2013 of 7 August 2013 does not contain restrictions to the use of non-mammalian embryos.

3.2. Tissue Collection

Embryos were obtained from fertilized chicken eggs which were purchased from commercial sources. The eggs were kept in a 37°C incubator, with 49% humidified atmosphere, for 4.5 to 5.5 days. Embryonic chick lungs were dissected using a stereomicroscope (Olympus SZX16, Japan), and staged (b1, b2 or b3) depending on the number of secondary buds present (1, 2 or 3, respectively). Additionally, whole chick embryos were collected and staged according to Hamburger and Hamilton (HH) developmental table (1951) (Hamburger and Hamilton 1951); embryos were used as positive controls for *in situ* hybridization, to validate that the procedure was performed correctly. Whole lungs were processed either for *in vitro* lung explant culture, *in situ* hybridization or protein extraction.

For *in vitro* lung explant culture, fresh lungs were immediately used to proceed with culture (section 3.3).

For *in situ* hybridization, whole lungs and embryos were immediately fixed in a 4% formaldehyde solution (2 mM EGTA in PBS pH 7.5), and stored at 4°C, overnight. Subsequently, tissues were dehydrated in PBT (PBS with 0.1% Tween 20) with increasing concentrations of methanol and stored at -20°C (section 3.4).

For protein extraction, fresh lungs were collected on ice, to prevent degradation by proteases, grouped in pools (6 lungs per stage/pool), and snap frozen in liquid nitrogen and stored at -80°C until further use (section 3.5).

3.3. Lung Explant Culture

During *ex vivo* culture, specific tissues or organs removed from an embryo are grown *in vitro* thus allowing observations and manipulations at a particular developmental window. With this technique, it is possible to manipulate the culture medium by adding molecules/compounds of interest and then examine their

impact on organ development. In this particular case, lung explants were grown *in vitro* on top of porous polycarbonate membranes and the culture medium supplemented with an inhibitor of YAP-TEAD interaction, hence interfering with canonical Hippo signalling pathway.

The medium preparation and tissue culture procedures were conducted in a sterile laminar flow tissue culture hood. Briefly, polycarbonate membranes (Nucleopore; Whatman, USA) were primarily soaked into 400 µl of 199 Medium (Sigma, USA) for at least 1 hour in a 24-well tissue culture plastic plate, at room temperature. Afterwards, 199 Medium was replaced with 200 µl of 199 Medium supplemented with 5% heat-inactivated fetal calf serum (Gibco, USA), 10% chicken serum (Gibco), 1% L-glutamine (Gibco), 1% penicillin 5000 IU/mL plus streptomycin 5000 IU/mL (Gibco) and 0.25 mg/mL ascorbic acid (Sigma) (lung medium). Stage b2 lungs were then carefully transferred onto previously soaked membranes and incubated for 30 minutes at 37°C, 5% CO_2. After this incubation period, explants were randomly assigned to one of the four experimental groups: DMSO (0.3%) or Verteporfin (Sigma) (5, 7.5 and 10 µM). Since VP was dissolved in DMSO (Sigma), DMSO-treated explants were used as the control for this experiment. Explants were incubated for 48 hours, at 37°C, 5% CO_2, and the medium replaced after 24 hours. Lung explant growth was recorded by photographing the lung explants, with an Olympus DP70 camera coupled to the stereomicroscope, at a day 0 (0h), day 1 (24h) and day 2 (48h). At D2, and after photographing the explants, lungs were pinched (to avoid accumulation of reagents) and processed for *in situ* hybridization as previously described (section 3.2).

In parallel, a different set of lungs (b1, b2, and b3 stage) were cultured in lung medium as described above, then gathered into pools (6 lungs/pool) for protein extraction (section 3.2) and subsequent western blot analysis (section 3.5).

3.3.1. Morphometric analysis

At 0h (D0) and 48h (D2), epithelial and mesenchymal perimeter and area, and total lung area were measured, in the images, with AxioVision Rel. 4.9.1 (Carl Zeiss GmbH, Germany). D0 and D2 lung explants were manually outlined allowing the program to compute the following variables: epithelial, mesenchymal and total area, as well as epithelial and mesenchymal perimeter. Additionally, the number of emerged secondary bronchi at D0 and D2 was calculated to assess branching. The results of the morphometric/branching analysis were represented as D2/D0 ratio and reflect lung growth. Statistical analysis was performed using SigmaStat 3.5 (Systat Software Inc., USA). For morphometric and branching analysis, all data passed normality and equal variance tests. Subsequently, One Way ANOVA

and Fisher LSD Method for pairwise multiple comparison was applied. The power was set to 0.050. Data are presented as mean ± SEM, and statistical differences set at $p<0.05$.

3.3.2. Medium collection for LDH assay

After 24h (D1) and 48h (D2) of lung explant culture, the medium from control (DMSO) and VP-treated groups was collected for LDH assay (section 3.6). The approximate volume of 200 µL was aspirated from each well. Afterwards, the medium was centrifuged at 1000 g for 20 min at 4°C. Subsequently, 50 µL aliquots were prepared and then stored at -80°C. In addition, lung medium (D0, not used in culture) was processed similarly to be used as negative control.

3.4. Whole Mount *In situ* Hybridization

In situ hybridization is a semi-quantitative technique which detects messenger RNA (mRNA) and reveals spatial localization and expression levels of specific mRNAs. This technique relies on the use of an antisense RNA probe labeled with different tags as, for instance, digoxigenin (DIG), which eventually binds to the mRNA of interest in the tissue. Afterwards, the RNA hybrid is detected in the tissue through the use of an antibody that recognizes the particular label. Ultimately, an enzyme bound to the antibody will complete a colorimetric reaction that determines the sites of expression.

3.4.1. Probe preparation

Total RNA was extracted from HH24 embryos using GRS Total RNA Kit (Grisp, Portugal). Subsequently, cDNA was synthesized with GRS cDNA Synthesis Kit (#GK24.0050; Grisp). The quality of generated cDNA was confirmed by conventional PCR (KAPA2G Fast ReadyMix PCR kit; KapaBiosystems, USA) with the amplification of a housekeeping gene (GAPDH). Specific oligonucleotides were designed to obtain part of the coding region of *lats1*, *lats2*, *mst1*, *mst2*, *yap*, *taz*, *tead1*, and *tead4* (Table 1).

After cDNA amplification by conventional PCR, fragment size was confirmed by agarose gel. Afterwards, the fragments with the expected size were inserted into a vector (pCR™II-TOPO®, Thermo Scientific, USA) containing T7 and Sp6 promoters. The above-mentioned procedures were performed according to the manufacturer's instructions.

The plasmid constructs were transformed by heat shock protocol (Ref: sambrook) into a specific strain of competent Escherichia coli (XL1-blue) cells, plated in Luria broth (LB) agar plates (0.5% yeast extract, 1% NaCl, 1% tryptone, 2% agar) supplemented with 0.1 mM IPTG (NZYTech, Portugal), 20 µg/mL X-gal (Nzytech) and 1 µg/mL ampicillin, and kept overnight at 37°C . Afterwards, the individual colonies were

Table 1: Primers sequences for the amplification of Hippo signalling genes by conventional PCR. The accession number represents the nucleotide sequence used to obtain primers. Primers forward (FW) and reverse (RV) were designed with Primer-BLAST online tool (NCBI); the expected product size (bp) and annealing temperature (^{O}C) were determined.

Gene	Accession number	Primer Sequence	Product Size (bp)	Annealing T(°C)
mst1_Fw	NM_001030853.1	CGTGAGCTGGATCAGGAAGATG	238-292	52
mst1_Rev		GCATCGTTTCATCCCTCCTTT		
mst2_Fw	NM_001031337.2	TTAACACTGAAGGCCATGCAA	472	51,1
mst2_Rev		TCTTCTAGTTCCCTCTGCTGC		
lats1_Fw	XM_025149311.1	AAGATGAAGAACGGCGGGAG	981	54,2
lats1_Rev		GAGGCTGGCCCACTAACATT		
lats2_Fw	XM_015279299.2	CAAGCATTTGTTAATTCCCGGCAG	400	53,3
lats2_Rev		CATTTGCTCCTGTTCTGCTTCAC		
yap1_Fw	NM_205243.1	CTGATGATGTACCTCTGCCACC	430	52,8
yap1_Rev		ACGGGATTTTGAGATCCACCA		
taz_Fw	XM_003641786.3	GGACAGCGTTACTTCCTCAATC	257	52,4
taz_Rev		GCACTGGGCATGTTCAGCAA		
tead1_Fw	NM_001199405.1	AGCGATTCTGCAGATAAACCTATTG	1026-1299	50
tead1_Rev		TTAGTCCTTTACAAGCCTGTAGATATG		
tead4_Fw	NM_204771.1	TTGGAGCTTCTAGCTGGCACCATTACCTCC	1170-1344	59,3
tead4_Rev		TAGTCTCTAGTCCTTCACCAGCCGGTAG		

screened by "Blue-White" selection. The selected white bacterial colonies, potentially containing the fragment of interest, were inoculated in liquid LB (0.5% yeast extract, 1% NaCl, 1% tryptone) with ampicillin for overnight culturing at 37°C with 220 rpm agitation. Eventually, the plasmid DNA was isolated using an Alkaline Lysis protocol (according to: Green and Sambrook, 2012). After a conventional PCR using M13 universal primers, size was confirmed with agarose gel electrophoresis (0.8%). The bacterial colonies containing the insert with the correct size were inoculated in 6 ml of liquid LB with ampicillin and cultured overnight as described above. On the following day, glycerol stocks were generated, and plasmid DNA was extracted using GeneJET Plasmid Miniprep Kit (Thermo Scientific), according to the manufacturer's instructions. This commercial kit relies on the presence of specific silica membrane, in which the plasmid DNA will firstly bind and then will be eluted. To assess plasmids integrity, an agarose gel electrophoresis was carried out. Additionally, plasmid DNA concentration was determined by NanoDrop spectrophotometer (NanoDrop ND-1000, USA) and sample purity was estimated based on the 260/280 ratio.

Finally, plasmid DNA was sent for sequencing (GATC Sequencing Service, Germany). Based on the sequencing results, the orientation of the insert and the RNA polymerase required for *in vitro* transcription to produce an antisense RNA probe were determined.

On the other hand, *ctgf* probe was kindly provided in filter paper by Dr. C. Lorda-Diez (Lorda-Diez et al. 2011). Briefly, the plasmid was eluted using ultrapure water and left at room temperature, for 2 hours. Next, the plasmid was transformed and plated, with ampicillin, as previously described. Subsequently,

selected isolated colonies were inoculated in liquid medium, overnight, and plasmid DNA was extracted and quantified as described above.

3.4.2. RNA Probe Synthesis

Firstly, the fragments of interest were obtained by PCR amplification (NZYTaq 2x Green Master Mix; NZYTech) using M13 universal primers. Afterwards, the agarose gel electrophoresis (0.8%) was performed. Once the expected size was confirmed, the DNA bands were excised directly from the gel and placed into previously scaled eppendorfs. Afterwards, the tubes with the gel were weighed again and subtracted the weight of an empty eppendorf, hence obtaining the weight just of the gel. Eventually, the DNA isolation was performed using commercial GF-1 Gel DNA Recovery Kit (Vivantis Technologies, USA) according to manufacturer's instructions. The purified DNA fragments were quantified using the NanoDrop spectrophotometer.

3.4.2.1. *In vitro* transcription

RNA antisense probes were obtained through an *in vitro* transcription reaction using approximately 750 ng of the purified fragment as template. For the *in vitro* transcription reaction, specific RNA polymerases (Table 2) and a nucleotide mix containing uracil bound to DIG was used (Roche Applied Sciences, USA). This molecule is the key for the detection procedure of *in situ* hybridization since it is recognized by an anti-DIG antibody coupled to an enzyme (alkaline phosphatase) that, in the presence of specific substrates, produces a blue precipitate (section 3.4.3, Detection).

Table 2: RNA polymerases used for *in vitro* transcription reaction selected to produce an antisense mRNA probe.

Gene	RNA polymerase
mst1	Sp6
mst2	T7
lats1	Sp6
lats2	T7
yap1	Sp6
taz	Sp6
tead1	T7
tead4	Sp6

3.4.3. In situ Hybridization procedure

3.4.3.1. Tissue permeabilization and hybridization

In situ hybridization procedure was performed according to Henrique et al. protocol with minor modifications (Henrique et al. 1995). At first, the whole lungs (n≥10/gene/stage), lung explants (n≥5/gene/culture condition) and embryos (n=2/gene) were rehydrated through a series of methanol into PBT at room temperature. Subsequently, tissues were treated with Proteinase K (20 mg/mL PBT). Proteinase K (Roche Applied Sciences) is a non-specific endopeptidase that cleaves peptide bonds from membrane proteins, and thus permeabilize the membrane enabling the entrance of the probe inside the cell. The incubation period must be carefully controlled and depends on the size of the tissue: 2 minutes for lung tissue and 35 minutes for HH25 embryos. In fact, the incubation time for whole embryos depends on their embryonic stage.

After several washes with PBT, to completely remove Proteinase K, tissues were treated with a fixing solution (10% formaldehyde, 0.4% glutaraldehyde in PBT pH 7.5) at room temperature. Eventually, tissues were washed to gradually move to hybridization solution (50% formamide, 1.3x SSC, 5 mM EDTA, 50 µg/ml tRNA, 0.2% Tween, 0.5% CHAPS, 100 µg/ml heparin) and were ultimately incubated for at least 1 hour at 70°C with hybridization solution. At last, tissues were incubated overnight, at 70°C, with DIG-RNA labeled probe mixed in the hybridization solution at a final concentration of 0.5%. During this overnight incubation period, RNA probe hybridizes to the corresponding mRNA in the tissue.

3.4.3.2. Addition of anti-digoxigenin antibody

The next day, tissues were abundantly washed with hybridization solution, pre-heated at 70°C overnight, to remove unbound or non-specifically bound probe. Afterwards, tissues were treated with blocking solutions, to reduce background by preventing the antibody from binding to non-specific sites and incubated overnight at room temperature with an anti-digoxigenin antibody (1/2000; Roche Applied Sciences) that will recognize DIG-labeled probe.

3.4.3.3. Detection

After overnight incubation with anti-digoxigenin antibody, tissues were exposed to series of washes in MABT (NaCl 750 mM, Maleic acid 500 mM, Tween 0.5%), which purpose is to wash away the excess of antibody and to reduce background staining. Then, lung tissues and embryos were washed several times with alkaline phosphatase buffer (NTMT) (Tris-HCl 100 mM at pH 9.5, $MgCl_2$ 50 mM, NaCl pH 5 100 mM, 0.1% Tween) followed by incubation with developing solution (NTMT + NBT + BCIP), in the dark, at

37°C. The antisense RNA probes are detected indirectly through enzyme-substrate interaction, where an anti-digoxigenin antibody is coupled with alkaline phosphatase, which in the presence of the substrates NBT/BCIP (Roche Applied Sciences) produces a blue precipitate.

3.4.3.4. Cross-section Preparation

Selected hybridized lungs were processed for slide sectioning. Briefly, tissues were dehydrated through a series of ethanol and embedded in 2-hydroxyethyl methacrylate (Heraeus Kulze, Germany). Subsequently, 25 µm sections were obtained with a rotary microtome (Leica RM 2155, Germany). Lung sections were photographed with a microscope (Olympus BX61) integrated with Olympus DP70 camera.

3.5. Western blot

Western blot is a qualitative and semi-quantitative technique that allows protein detection in homogenates by first separating the proteins by size (gel electrophoresis) and subsequent transfer to a blotting membrane. The membrane-bound proteins are then detected using antibodies that recognize the protein of interest, and then enzyme-conjugated secondary antibodies that distinguish the primary host species, which in the presence of substrate result in the formation of a chemiluminescent product, which is then captured with a digital imaging system.

The pooled embryonic chick lungs at 0h (D0) and after 48h of culture (D2) were used for western blot assay. Three independent experiments per pool were performed.

3.5.1. Protein extraction

Protein extraction was performed according to Kling et al. protocol with minor modifications (Kling et al. 2002). 20 µl of ice-cold lysis buffer [(HEPES pH 7.5 20 mM, glycerophosphate 50 mM, EGTA 2 mM, 10% glycerol, sodium vanadate 1 mM, 1% Triton X-100, 1% complete protease inhibitor (Sigma)] was added to pooled tissue samples (6 lungs/pool). Tissues were homogenized on ice using a pellet pestle cordless motor (Kontes Glass, USA), during 3 cycles of 10 seconds at maximum speed followed by 2 minutes on ice. Subsequently, the samples were centrifuged at 10000 rpm for 30 min at 4°, and the supernatant collected and stored at -80°C.

The protein concentration was determined using the Bradford method for Protein Assay (Bio-Rad, USA), according to the manufacturer's instructions. Bovine serum albumin was used as a standard (Protein Assay Kit II, Bio-Rad) and prepared in different dilutions (0.1, 0.2, 0.3, 0.5, 0.7 mg/ml). Each cuvette contained 20 µl of each standard and 1 ml of diluted dye. The standards were incubated at room

temperature for 5 min and then measured at 595nm (T80+ US/VIS spectrophotometer; Oasis Scientific Inc, USA). A calibration curve was obtained by applying a linear regression. Next, 1 µl of each sample was incubated and measured as previously described. Finally, the concentration of total protein was determined by the linear regression equation.

3.5.2. Protein separation by electrophoresis (SDS-PAGE)

Proteins were separated by size using SDS-PAGE gel from a commercial kit (TGX Stain-Free FastCast acrylamide, Bio-Rad) and according to manufacturer's indications. The gels were cast in 0.75 mm glass plates (Bio-Rad). Ten µg of total protein were prepared with a commercial Laemmli buffer ((#1610737, Bio-Rad) mixed with β-mercaptoethanol (Sigma) and heated at 95-100°C for 15 min. Finally, the protein samples were loaded into SDS-PAGE gel submerged in 1x running buffer (Tris-base 24.77 mM, glycine 191.82 mM, SDS 3.46 mM, pH 8.3) and run at 100 V, for approximately 2 hours. The protein size was evaluated according to molecular weight marker (ThermoFisher Scientific, USA).

3.5.3. Protein transfer

First, the gel and nitrocellulose membrane (Hybond-C Extra, GE Healthcare Life Sciences, UK) were assembled between filter paper sheets. Then, the electrophoretic transfer was achieved by using the Trans-Blot® Turbo™ Transfer System (Bio-Rad) at 25V, 0.2A for 7 min and transfer buffer (Tris-base 25 mM, glycine 0.2 M, 20% methanol at pH 8.5).

3.5.3.1. Blocking and antibody incubation

The nitrocellulose membranes were washed with TBS-T (Tris 200 mM, NaCl 1.37 M, 0.1% Tween-20 pH 7.6) for 10 min. Afterwards, the membranes were blocked with blocking buffer (5% non-fat dry milk in TBS-T), for 2 hours at room temperature. Then, the membranes were washed 3 times with TBS-T, for 20 min. Eventually, the blotting membranes were incubated with primary antibodies: YAP (1:5000; #14074, Cell Signalling Technology, USA), YAP-Ser127 (1:5000; #13008, Cell Signalling Technology) and β-tubulin as loading control (1:200000; #ab6046, Abcam Inc., UK). The antibodies were diluted in 5% BSA in TBS-T and left overnight at 4°C. Then the membranes were washed 3 times with TBS-T for 20 min at room temperature followed by incubation with anti-rabbit secondary antibody HRP-conjugated with horseradish peroxidase (HRP) (1:2000; #7074, Cell Signalling Technology) in 2% non-fat dry milk in TBS-T, at room temperature for 1 hour, and again exposed to several washes with TBS/T for 20 min.

3.5.3.2. Detection and analysis

Clarity Western ECL Blotting Substrate (Bio-Rad) was used for signal development. This substrate was used according to the manufacturer's instructions. The chemiluminescent signal was captured using the Chemidoc XRS (Bio-Rad).

Quantitative analysis was performed with ImageLab software (Bio-Rad). Each protein band was normalized to their corresponding β-tubulin (control). Statistical analysis was performed, using SigmaStat 3.5 (Systat Software Inc.). pYAP/YAP ratio was assessed at Day 0 (0h) and Day 2 (48h). At first the normality and equal variance tests were applied and successfully passed. Subsequently One Way ANOVA test was used, which did not detect statistical differences in Day 0 ($p=0.171$) and in Day 2 ($p=0.486$). The power was set to 0.050. The data are presented as mean ± SEM.

3.6. Lactate dehydrogenase assay

The lactate dehydrogenase (LDH) is a stable enzyme present in the cytosol but leaked into extracellular space (culture medium) upon plasma membrane damage. Eventually, the presence of LDH enzyme in the medium is a good measurement of plasma membrane integrity and consequently cell damage. To assess the possible cytotoxic effect of VP in lung explants, LDH levels were assessed, in the culture medium, using Lactate Dehydrogenase Activity Colorimetric Assay Kit (#K726-500, Biovision, USA) as per manufacturer's instructions.

The culture media was collected from control and VP treated groups (5, 7.5 and 10 μM) (see section 3.3.2). Lung medium was used to discard LDH activity within the media itself. In brief, the NADH standard curve was prepared with the following concentrations 0, 2.5, 5.0, 7.5, 10.0 and 12.5 nmol, maintaining the final volume of 50 μl with Assay Buffer. The positive control was provided from the kit. The sample media was diluted in the ratio 1/250 in 50 μl of Assay Buffer and transferred into 96-well plates. Each sample or standard was run in duplicate. Finally, 50 μl of Reaction Mix was added to each well and the OD (optical density) was recorded with a spectrophotometer (Varioskan™ LUX multimode microplate reader, Thermo Scientific, USA) at 450 nm. The baseline measurement was taken at 0 min (T0) and after 30 min (T1).

3.6.1. Data analysis

The standard curve was plotted (OD *vs* NADH) considering only the average values obtained after 30 min of incubation. NADH background (0 nmol) was deducted from all the standards.

For samples, ΔA (T1 – T0) was calculated and, also, average values were used. To eliminate lung medium background, ΔA from lung medium (D0) was subtracted to ΔA of all samples. To determine the amount of NADH generated (B value) between T1 and T0, the sample ΔT450 nm was applied to the NADH standard curve:

LDH Activity=B/((T1-T0) x V) X Sample dilution= nmol/min/ml = mU/ml

4.RESULTS

HIPPO signalling is involved in numerous cellular events as, for instance, organ growth control (Yu et al. 2015; Wang et al. 2017; Moya and Halder 2016). The mammalian HIPPO core components are: MST1/2 and LATS1/2 (main kinases); SAV1 and MOB1A/1B (co-factors); YAP and TAZ (transcriptional co-activators); TEAD1-4 (transcription factors). Briefly, if YAP/TAZ is phosphorylated it is retained in the cytoplasm; on the contrary, unphosphorylated YAP/TAZ translocate to the nucleus thus activating the transcription of HIPPO target genes such as *ctgf* (Kanai et al. 2000; Zhao et al. 2007; Zhao et al. 2010; Wang et al. 2016)(Guo and Teng 2015; Woodard et al. 2017; Yeung et al. 2016). HIPPO kinase cascade and phospho-activation of YAP/TAZ have already been described in different organ systems (Moya and Halder 2016; Patel et al. 2017; Wang et al. 2017) and, it has been shown that it regulates growth differently, depending on the organ (Gao et al. 2013; George et al. 2012; Camargo et al. 2007). Regarding the developing lung, there are still some gaps that need further examination.

The organogenesis of the respiratory system depends on well-coordinated multiple signalling pathways (Ornitz and Yin 2012) and, recently, it has been suggested that YAP is involved in proliferation, patterning, and differentiation of airway progenitors (Mahoney et al. 2014; Lange et al. 2015). Nonetheless, it needs additional study to better comprehend the mechanisms underlying lung growth control. In this sense, in this work we aimed to fully characterize HIPPO signalling machinery and its role in early stages of lung development, using the chicken as a model.

For this purpose, the spatial localization of HIPPO signalling components, in early stages of chick lung development, was determined by whole mount *in situ* hybridization, namely: *mst1*, *mst2*, *lats1*, *lats2*, *yap, taz, tead1, tead4,* and *ctgf*. Additionally, protein expression levels of pYAP and YAP were assessed to determine if HIPPO signalling is active in the embryonic chick lung. Afterwards, using *in vitro* lung explant culture, HIPPO pathway was modulated with verteporfin (VP). HIPPO modulation was confirmed by assessing *ctgf* expression levels, by *in situ* hybridization. Furthermore, explants were morphometrically analysed to determine the impact of HIPPO manipulation on lung growth. Finally, LDH cytotoxicity was performed to assess tissue damage.

4.1. Characterization of expression pattern of Hippo signalling members during chick lung development

To establish the expression profile of HIPPO signalling pathway in early stages of chick lung development (b1, b2 and b3), whole mount *in situ* hybridization for *mst1*, *mst2*, *lats1*, *lats2, yap, taz, tead1, tead4,*

and *ctgf* was performed. Subsequently, representative examples of hybridized lungs were processed for histological sectioning for more detailed analysis.

4.1.1. mst1 and mst2

mst1 expression is restricted to the pulmonary epithelium of developing chick lung, in the three stages studied (Figure 5a-c). However, it is absent from the distal-most epithelium of primary bronchi and tracheal epithelium (Figure 5c, black arrowhead; Figure 5a, section sign, respectively). The histological analysis confirmed the expression of *mst1* in the epithelium where the secondary bronchi arise (Figure 5d, open arrowhead), diminishing gradually at the distal-most epithelium of secondary branches (Figure 5d, asterisks). Even though the same expression pattern is maintained throughout the stage studied, the b1 staged lungs exhibited a weaker expression of *mst1* (Figure 5a).

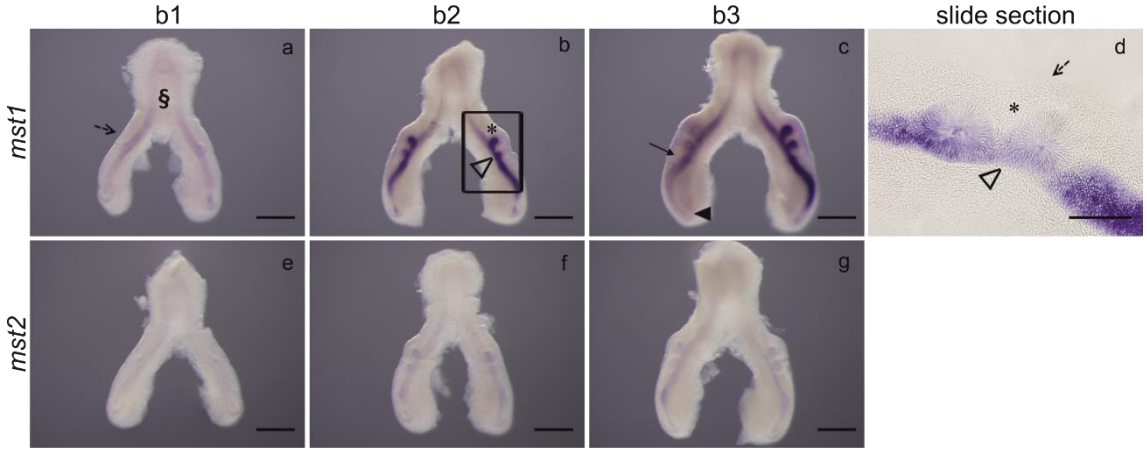

Figure 5. *mst1 and mst2* expression pattern in the early stages of avian lung organogenesis. Representative examples of whole mount *in situ* hybridization of stage b1, b2 and b3 lungs for: *mst1* (a-d) and *mst2* (e-g), n≥9 per stage. Scale bar: whole mount, 500 μm; slide section, 100 μm.
The black rectangle in image (b) indicate the region shown in corresponding slide section. *Asterisk* secondary bronchi. *Black arrowhead* distal epithelium. *Open arrowhead* sites of emerging secondary bonchi. *Black arrow* primary bronchi. *Section sign* trachea region.

Even after a long developing period, only a very weak expression of *mst2* was observed in the developing chick lung, in all stages studied (Figure 5e-g). For this reason, slide sectioning was not viable. It is worth mentioning, that this gene is present in the head and ventral region of HH 25 embryo (Annex I, Figure 1). Therefore, we can discard the possibility that an error could have occurred during the ISH procedure. Nonetheless, it is likely, that *mst2* is absent from the lung, but may be involved in the development of other vital organs.

4.1.2. lats1 and lats2

lats1 mRNA was detected in the mesenchymal compartment around the main bronchial tree (Figure 6a-c). In the mesenchyme, *lats1* expression becomes more intense around outgrowing secondary branches (Figure 6c and f, dashed arrow) and then extends in the ventral-distal direction (Figure 6a and b, dashed arrow). The histological analysis demonstrated weak expression in the epithelium of secondary branches (Figure 6d, asterisks). *lats1* mRNA was absent from the distal mesenchyme (Figure 6b, black arrowhead).

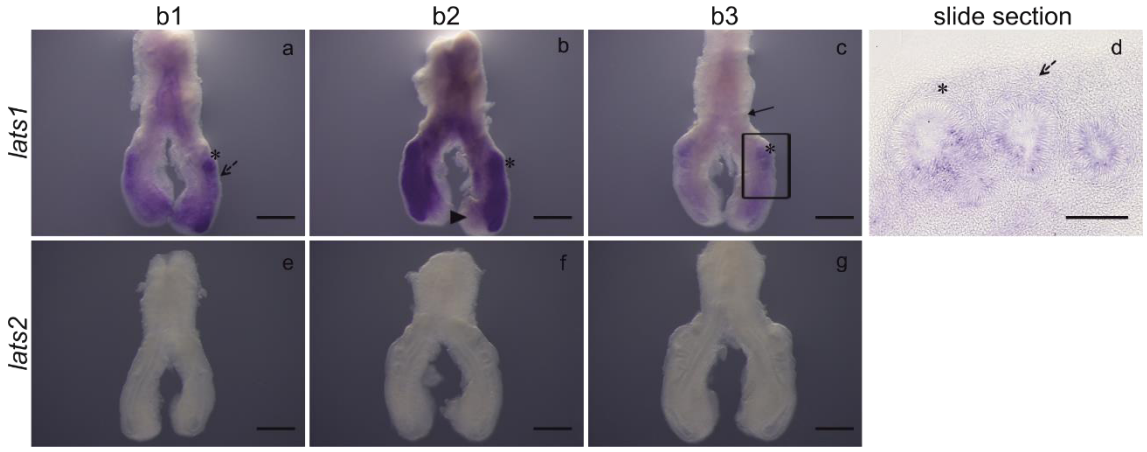

Figure 6. *lats1* and *lats2* expression pattern in the early stages of avian lung organogenesis. Representative examples of whole mount *in situ* hybridization of stage b1, b2 and b3 lungs for: *lats1* (a-d) and *lats2* (e-g), n≥9 per stage. Scale bar: whole mount, 500 μm; slide section, 100 μm. The black rectangle in image (c) indicate the region shown in corresponding slide section. *Asterisk* secondary bronchi. *Black arrowhead* distal mesenchyme. *Black arrow* primary bronchi. *Dashed arrow* mesenchyme.

The expression of *lats2* was not detected in developing chick lung, in all stages studied (Figure 6e-g). For this reason, slide sectioning was not viable. Nonetheless, weak expression in the head and the ventral-distal region was observed in HH 25 embryo (Annex I, Figure 2), further suggesting that this gene may have a lesser role (when compared to *lats1*) in early chick embryo development.

4.1.3. yap and taz

yap is ubiquitously expressed in the pulmonary mesenchyme in the three stages studied (Figure 7a-c). Further histological analysis revealed that *yap* mRNA is completely absent from all the epithelial compartment (Figure 7b, black arrow, and asterisks) bronchi. This pattern is maintained throughout all stages studied.

taz mRNA was observed exclusively in the pulmonary epithelium of the main bronchi (Figure 7e-g), specifically between the carina region and the distal region. It is expressed in the primary bronchi (Figure 7e and g, black arrow) accompanying the appearance of secondary branches (Figure 7h, open

arrowhead). Furthermore, *taz* is not detected in the epithelium of the trachea (Figure 7f, section sign), secondary bronchi (Figure 7h, asterisks) and distal tip (Figure 7f, black arrowhead).

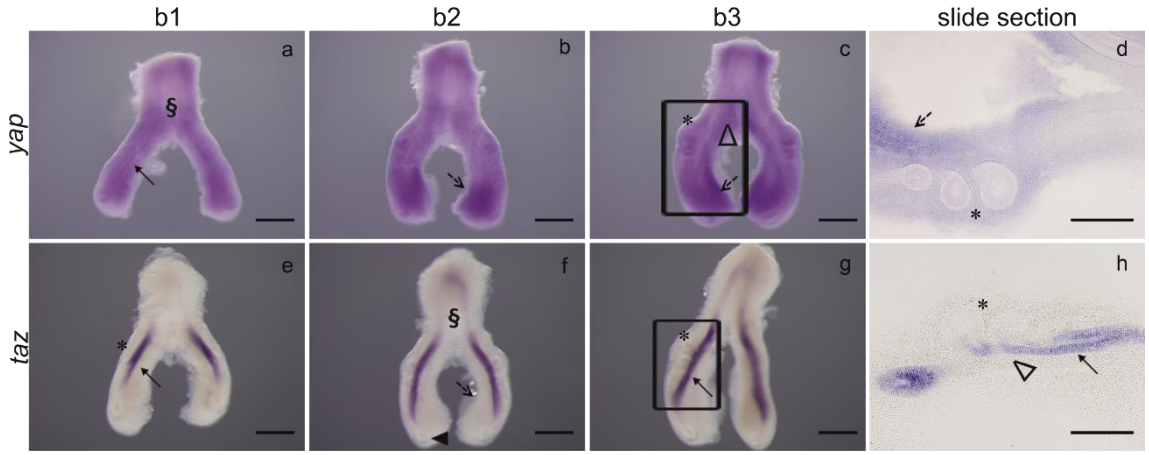

Figure 7. *yap* and *taz* expression pattern in the early stages of avian lung organogenesis. Representative examples of whole mount *in situ* hybridization of stage b1, b2 and b3 lungs for: *yap* (a-d) and *taz* (e-h), n≥9 per stage. Scale bar: whole mount, 500 μm; slide section, 200 μm. The black rectangle in image (c and g) indicate the region shown in corresponding slide section. *Asterisk* secondary bronchi. *Black arrow* primary bronchi. *Dashed arrow* mesenchyme. *Black arrowhead* distal epithelium. *Open arrowhead* sites of emerging secondary bonchi. *Delta sign* carina region. *Section sign* trachea region.

4.1.4. tead1 and tead4

tead1 transcript is present in the mesenchyme of the chick respiratory tract, especially in the dorsal region adjacent to the secondary bronchi and in the distal-ventral region (Figure 8b, dashed arrow) (Figure 8a-c); on the other hand, it lacks from the mesenchyme surrounding the trachea (Figure 8a, section sign) and distally (Figure 8b, black arrowhead). Slide sectioning revealed that *tead1* is not expressed in the pulmonary epithelium of primary (Figure 8d, black arrow) and secondary bronchi (Figure 8d, asterisks).

tead4 is expressed in pulmonary mesenchyme in early stages of the developing chick lung (Figure 8e-g). The expression is mainly evident around the trachea (Figure 8e, dashed arrow), in the carina region (Figure 8f, delta sign) and dorsal-ventral mesenchyme around secondary branches (Figure 8f, dashed arrow). The histological analysis confirmed this pattern, but it also revealed that *tead4* is absent from the epithelial compartment (Figure 8h, black arrowhead and asterisks, distal epithelium and secondary bronchi, respectively).

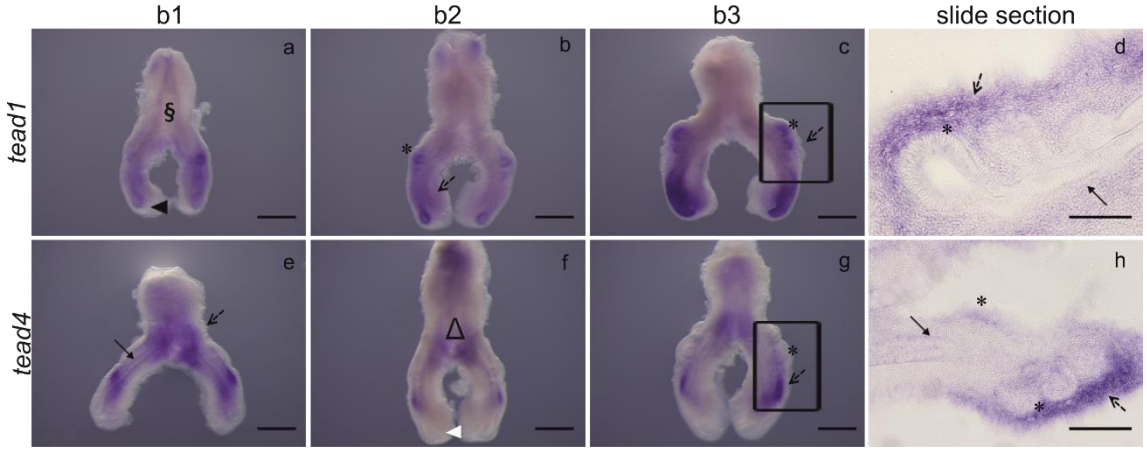

Figure 8. *tead1* and *tead4* expression pattern in the early stages of avian lung organogenesis. Representative examples of whole mount *in situ* hybridization of stage b1, b2 and b3 lungs for: *tead1* (a-d) and *tead4* (e-h), n≥9 per stage. Scale bar: whole mount, 500 μm; slide section, D, 100 μm; H, 200 μm. The black rectangle in image (c and g) indicate the region shown in corresponding slide section. *Asterisk* secondary bronchi. *Black arrowhead* distal mesenchyme. *White arrowhead* distal epithelium. *Black arrow* primary bronchi. *Dashed arrow* mesenchyme. *Delta sign* carina region. *Section sign* trachea region.

4.1.5. ctgf

ctgf is detected in the distal-ventral region of pulmonary mesenchyme (Figure 9b and c, dashed arrow). *ctgf* seems to be weakly expressed in the tracheal epithelium (Figure 9a, section sign), main bronchus (Figure 9b, black arrow) and peripheral airway buds (Figure 9c, asterisks). The histological analysis confirmed, this pattern (Figure 9d, asterisks, and black arrow) and further revealed vascular type line in the distal-ventral mesenchyme (Figure 9d, dashed arrow). *ctgf* mRNA was not detected in the distal tip of the primary bronchus (Figure 9a, black arrowhead) and distal-dorsal mesenchyme (Figure 9c, dashed arrow).

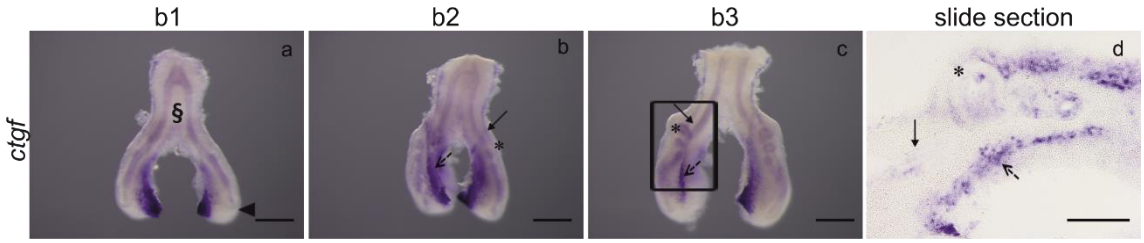

Figure 9. *ctgf* expression pattern in the early stages of avian lung organogenesis. Representative examples of whole mount *in situ* hybridization of stage b1, b2 and b3 lungs for: *ctgf* (a-d), n≥9 per stage. Scale bar: whole mount, 500 μm; slide section, D, 100 μm. The black rectangle in image (c) indicate the region shown in corresponding slide section. *Asterisk* secondary bronchi. *Black arrowhead* distal epithelium. *Black arrow* primary bronchi. *Dashed arrow* mesenchyme. *Section sign* trachea region.

In table 3, a summary of expression pattern of all genes is presented.

Table 3: Summary of gene expression pattern of Hippo pathway members and target

	Genes								
	mst1	***mst2***	***lats1***	***lats2***	***yap***	***taz***	***tead1***	***tead4***	***ctgf***
Mesenchyme									
trachea	-	-	+	-	++	-	-	+	++ (vascular)
secondary bronchi (dorsal)	-	-	++	-	++	-	++	++	-
distal-ventral	-	-	++ (except distal)	-	++	-	++ (except distal)	++ (except distal)	++ (vascular)
Epithelium									
trachea	-	-	-	-	-	-	-	-	+
main bronchi	++ (except distal)	-	-	-	-	++ (except distal)	-	-	+ (except distal)
secondary bronchi	++ (except distal)	-	+	-	-	-	-	-	+ (except distal)

- no expression, + weak expression, ++ strong expression

4.2. Hippo signalling activity in early branching stages of embryonic chick lung

YAP phosphorylation status is directly related with the activity of HIPPO signalling pathway. The balance between YAP (nuclear) and phosphorylated-YAP (cytoplasmic) protein levels, is associated with the ability to activate (or not) the transcription of specific target genes. In this sense, to determine whether the embryonic lung possesses the protein machinery necessary to convey HIPPO cellular responses, phosphorylated-YAP (pYAP) and YAP expression levels were assessed by western blot. For instance, if the pYAP/YAP ratio is below 1, it indicates that the nucleic/active form is more represented than cytoplasmic/inactive thus promoting transcription of HIPPO target genes.

For this purpose, the basal expression levels of YAP and pYAP were evaluated in early branching stages (b1, b2, and b3 stage). Additionally, the expression levels of both forms were also evaluated after culturing lungs *in vitro* for 48 hours, in normal explant conditions (Figure 10).

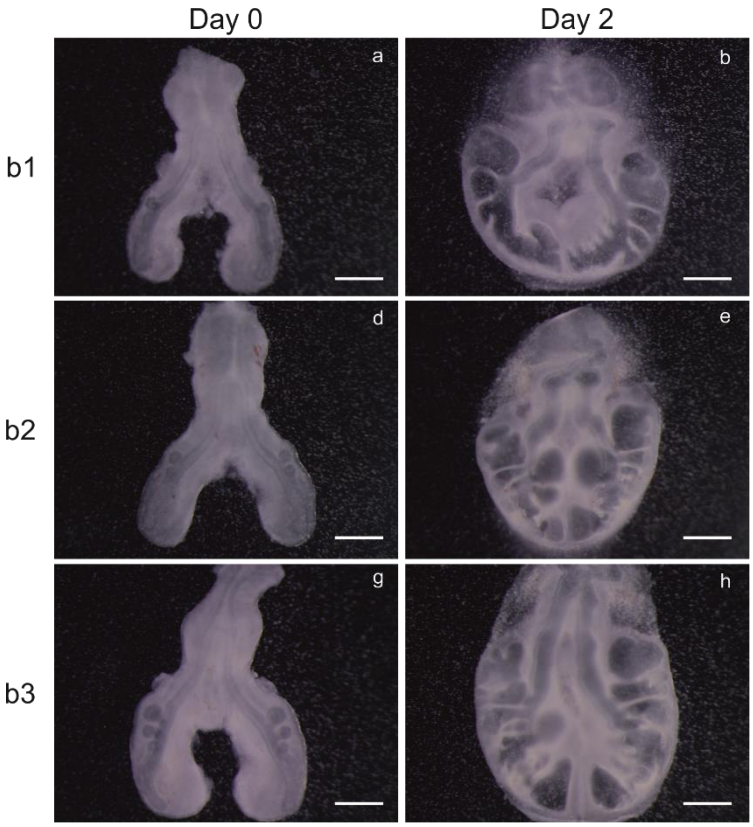

Figure 10. *In vitro* chick lung explant culture. Representative examples of stage b1, b2 and b3 lungs at 0h/D0: 0 h (a, c, e) and 48h/D2: 48 h (b, d, f) of incubation. Scale bar: a-f, 500 µm.

With this approach, the pYAP/YAP ratio was determined at two time points: basal (which means before culture: 0 hours, D0) and after culture (48 hours, D2). This ratio can be used as an indicator of HIPPO pathway activity.

In figure 11a, a representative example of a western blot for both proteins and time points is displayed. β-tubulin serves as a loading control. The expression levels of both YAP and pYAP seem very similar in the basal (D0) condition, in the three stages studied. However, the expression levels of both proteins declined, equally, after 48h of culture (Figure 11a).

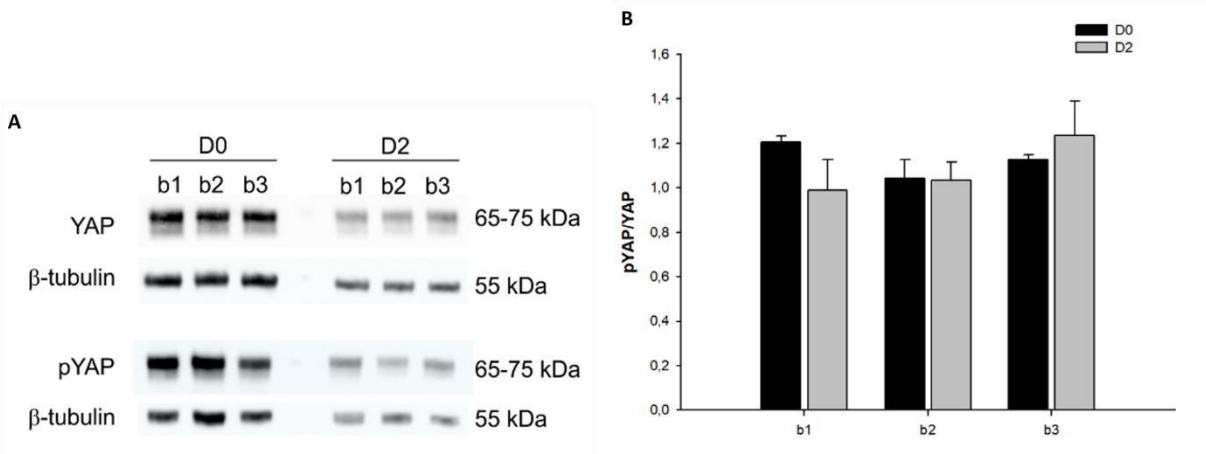

Figure 11. YAP and pYAP expression levels in the embryonic chick lung. (A) Western blot analysis of YAP and pYAP in stages b1, b2 and b3 at 0 (D0) and 48 hours (D2). β-tubulin was used for loading control (55 kDa). Both YAP and pYAP correspond to 65-75 kDa. (B) Semi-quantitative analysis for pYAP/YAP ratio at 0 (D0) and 48 hours (D2). The results are presented in arbitrary units normalized for β-tubulin. $p<0.486$.

Semi-quantitative analysis revealed that, at 0 h, pYAP and YAP protein levels are identical which means that pYAP/YAP ratio is similar amongst all stages, with the values between 1 and 1.2. After 48 h of culture, this ratio exhibits a minor, and non-significant increase, from b1 to b3 stage but is maintained approximately 1 (Figure 11b). These findings suggest a steady/proportional regulation of both forms of YAP (inactive and active) during early branching stages implying that HIPPO signalling pathway is active in this tissue.

4.3. *In vitro* Hippo manipulation in the embryonic chick lung

To clarify the role of HIPPO signalling pathway during early stages of chick lung branching, *in vitro* manipulation of HIPPO was performed. Chick lung explants were treated with different doses of Verteporfin (VP). This compound prevents YAP-TEAD association resulting in impaired transcription of HIPPO target genes (Al-Moujahed et al. 2017) thus mimicking HIPPO activation ("ON" status). For this

reason, HIPPO manipulation was confirmed, by *in situ* hybridization, for *ctgf* and its impact on pulmonary growth assessed by morphological analysis.

4.3.1. Validation by in situ hybridization for ctgf

Stage b2 lungs were cultured, for 48 h, with DMSO (control) or with different doses of verteporfin (5, 7.5 and 10 µM) (Figure 12). It seems that explants treated with 7.5 and 10 µM of VP (Figure 12h and 12k, respectively) displayed a decrease in the overall size of the lung when compared to control (Figure 12b). On the other hand, 5 µM of VP-treated lungs (Figure 12e), did not exhibit evident morphological differences when compared to control.

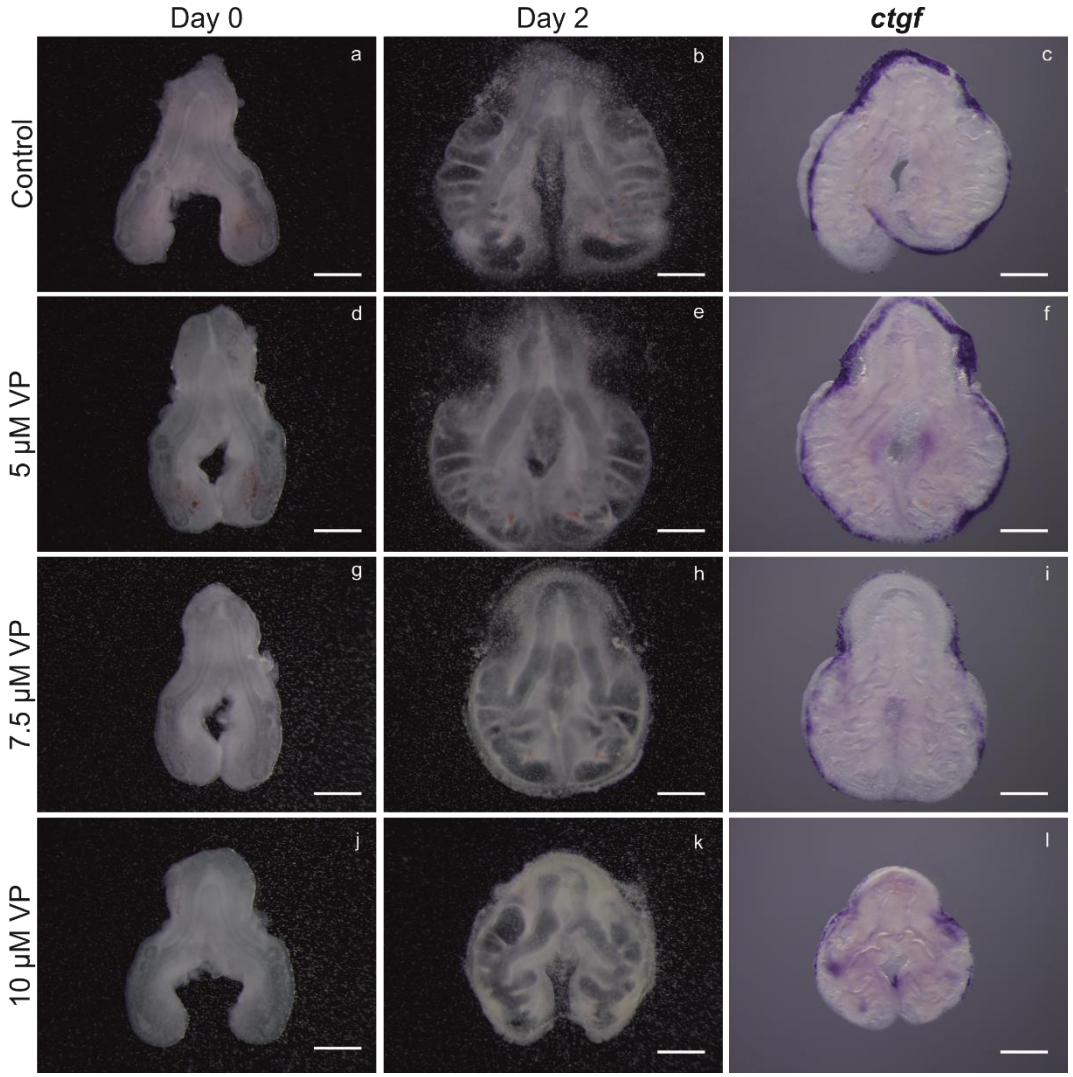

Figure 12. *In vitro* lung explants cultured with YAP-TEAD inhibitor followed by *in situ* hybridization with *ctgf*. Depiction of b2 stage lung explants at 0h (a, d, g, j) and after 48h of culture (b, e, h, k) in control or VP supplemented media, followed by whole mount *in situ* hybridization for *ctgf* (c, f, i, l), n≥4 for each condition. Scale bar: a-l, 500 µm.

In situ hybridization for *ctgf* confirmed that VP effectively interfered with HIPPO signalling (Figure 12c, f, i, l). *ctgf* expression pattern in control explants is in accordance with gene characterization results described in the previous section (Figure 9a-d). No differences in *ctgf* expression levels between control and 5 μM of VP-treated lungs (Figure 12c and f) were observed, while explants exposed to 7.5 μM dose demonstrated only a minor decrease in *ctgf* mRNA levels (Figure 12i). However, 10 μM of VP-treated explants displayed a noticeable reduction of *ctgf* expression levels (Figure 12l) therefore confirming down-regulation of target gene transcription.

Collectively, these results imply, that morphological alterations observed in lung explants could be due to an impairment of HIPPO signalling.

4.3.2. Morphometric and branching analysis of embryonic chick lung

Lungs explants, at 0h and 48h, were assessed morphometrically by measuring a set of parameters that allow evaluating lung growth: total/epithelial/mesenchymal area and epithelial/mesenchymal perimeter. Additionally, the number of secondary buds was determined at the same time points to evaluate branching. Data is represented as D2/D0 ratio.

The branching analysis revealed that explants treated with 5 μM of VP branched similarly as control lungs (Figure 13). However, lungs treated with 7.5 and 10 μM of VP displayed a statistically significant reduction (approximately 15% and 40%, respectively) in branching when compared to both the control and 5 μM treated explants. This suggests, that higher doses of VP (7.5 and 10 μM) result in suppressed embryonic lung branching in a dose-dependent manner.

The morphometric evaluation showed that explants cultured in 5 μM of VP displayed a statistically significant reduction in total area, mesenchymal area, and perimeter (approximately 11, 23 and 7 % respectively), when compared to control. The lungs treated with 7.5 μM of VP supplemented medium, showed a statistically significant decrease in total and mesenchymal area (approximately 14 and 19 %), as well as epithelial and mesenchymal perimeter (approximately 11 and 9 %), when compared to control. While the lungs subjected to 10 μM of VP demonstrated a statistically significant decline in all parameters examined: total (31%), epithelial (37%) and mesenchymal (25%) area; epithelial (33%) and mesenchymal (22%) perimeter (Figure 14).

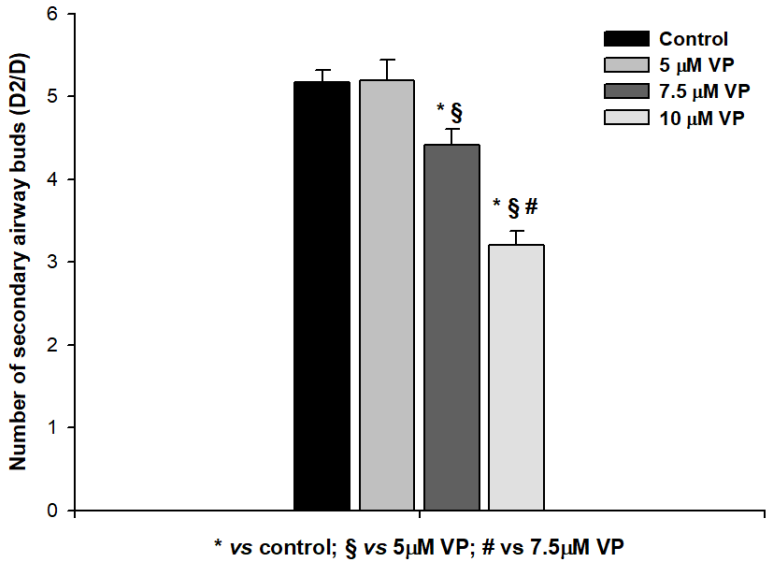

Figure 13. Branching analysis of lung explants. Control and VP treated (5, 7.5 and 10 µM) stage b2 lung explants (n≥10 for each condition) were evaluated at D0 and D2 for total number of secondary airway buds. Results are expressed as D2/D0 ratio. The data is shown as mean ± SD. p>0.05: ** vs* Control; § *vs* 5 µM VP; **#** 7.5 µM VP.

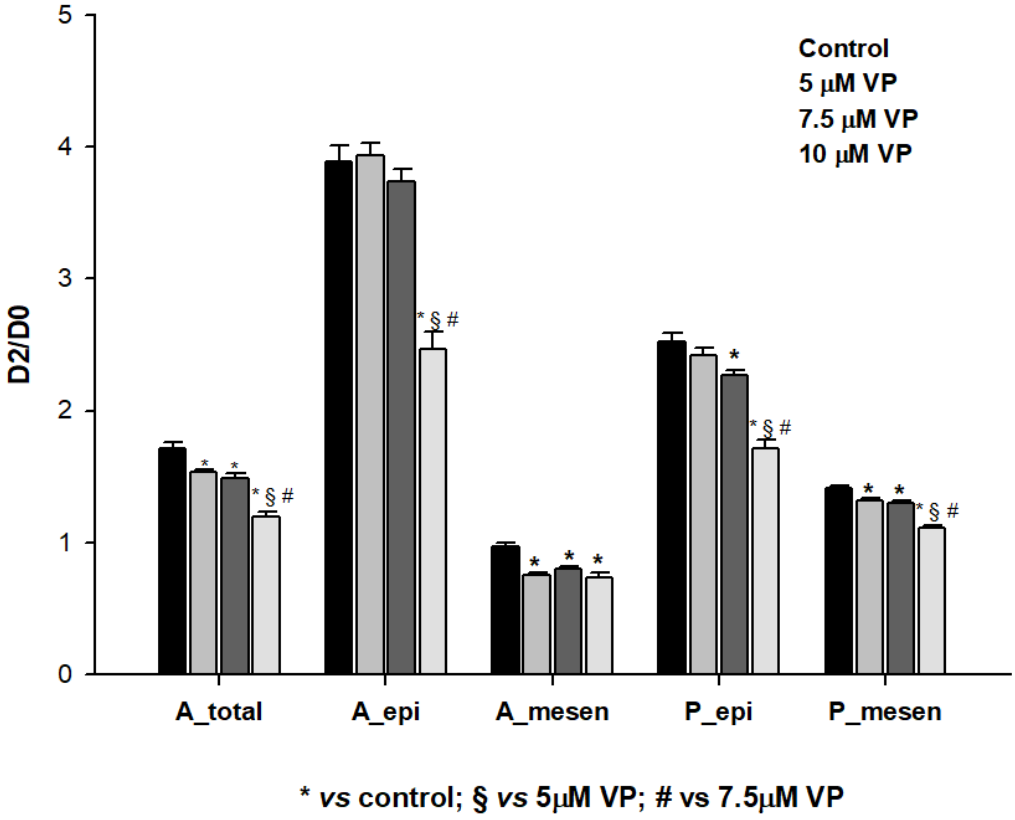

Figure 14. Morphometric analysis of lung explants. Control and VP treated (5, 7.5 and 10 µM) stage b2 lung explants (n≥10 for each condition) were evaluated at D0 and D2 for: total area (A_total); mesenchymal area (A_mesen); epithelial area (A_epi); mesenchymal perimeter (P_mesen); epithelial perimeter (P_epi). Results are expressed as D2/D0 ratio. The data is shown as mean ± SD. p>0.05: ** vs* Control; § *vs* 5 µM VP; **#** 7.5 µM VP.

4.3.3. Verteporfin-induced cytotoxicity in embryonic chick lung

Lung explants treated with increasing doses of YAP-TEAD inhibitor displayed a progressive impairment in growth that may be due, for instance, to increased cellular death. In this sense, cellular toxicity after 48 hours in culture was evaluated by lactate dehydrogenase (LDH) assay.

Lactate dehydrogenase (LDH) is a soluble but stable cytosolic enzyme. When the integrity of the plasma membrane is disrupted the intracellular content, namely LDH, is released to extracellular space. The increase in the number of membrane-damaged cells results in an increase in LDH activity in the surrounding environment, as for instance, in the culture media. In this case, culture medium collected at 24 (D1) and 48 (D2) hours was analysed to assess LDH activity; moreover, pre-culture lung medium (D0) was used as a control.

The results revealed that the control medium (D0) has a basal LDH activity. The LDH activity of both control and VP-treated conditions (5, 7.5 and 10 μM) was calculated by eliminating this effect and, ultimately, no LDH activity was detected suggesting that lung tissue may not be significantly altered.

5.DISCUSSION

Evolutionary conserved HIPPO molecular pathway is involved in tissue regeneration, cancer, and organ growth control. This signalling pathway is composed by a complex kinase cascade that ultimately regulates transcription of specific target genes responsible for conveying the adequate cellular response. Depending on the phosphorylation status and subcellular location of its main effector (YAP/TAZ) transcription may, or may not, be activated (Yu et al. 2015; Wang et al. 2017; Moya and Halder 2016; Woodard et al. 2017). The pulmonary development requires a tight regulation of numerous transcription factors and signalling pathways, such as SHH, WNT, FGF, and RA (Ornitz and Yin 2012). Coordinated signalling between epithelial and mesenchymal compartments is crucial for proper lung development. Recent studies suggest that HIPPO effector YAP is involved in proliferation, patterning, and differentiation of airway progenitors (Mahoney et. al. 2014), yet more profound investigation is required. The work presented in this Master thesis aims to dissect the role of HIPPO signaling pathway during early stages of chick lung branching by characterizing the main components of this kinase cascade and determining its function as a regulator of organ growth.

5.1. Expression pattern of *mst1*, *mst2*, *lats1*, *lats2*, *yap*, *taz*, *tead1*, *tead4* and *ctgf* in the embryonic chick lung

In this work, all experiments were performed in the embryonic chick lung that presents molecular and morphological similarities with mammalian, especially in the early stages of lung branching (Moura et al. 2011; Moura et al. 2014; Sakiyama et al. 2003). In order to study the expression pattern of HIPPO pathway components, embryonic chick lungs from b1, b2, and b3 stages were characterized by *in situ* hybridization. The spatial distribution of *mst1*, *mst2*, *lats1*, *lats2*, *yap, taz, tead1, tead4*, and *ctgf* were characterized, for the first time, in the embryonic chick lung.

- ***mst1* and *mst2***

mst1 is expressed in the epithelial compartment of primary bronchi where the secondary branches emerge (Figure 5d), whereas *mst2* expression was extremely faint. *mst1* and *mst2* are expressed in the mouse embryo from E8.5-E12.5, and play essential roles in placental development, vascular patterning, primitive hematopoiesis, and cell proliferation and survival (Oh et al. 2009). Conversely, the spatial distribution in the mammalian lung is not known. Nonetheless, different authors have addressed the role of MST1/2 in lung development; Lange et al. 2015 described that MST1/2 regulates lung development through conserved HIPPO/YAP signalling.

- ***lats1* and *lats2***

lats1 expression was detected in the mesenchymal compartment, especially surrounding the outgrowing secondary branches (Figure 6d). Conversely, we did not detect *lats2* transcript in the stages studied (Figure 6e-g). It is worth noting, that *in situ* hybridization for this gene was carried out several times to confirm the absence. In HH25 embryos, *lats2* seems to be expressed in the head and distal-ventral region, and absent from the limbs. It is possible that *lats2* is involved in the development of other organs, but not the lung.

It has been shown that mesenchyme-specific LATS1/2 double mutation leads to embryonic death at E14.0-E14.5 with mesenchymal gut overgrowth, suggesting that LATS kinase is mandatory for the development of gut mesenchyme (cotton2017). Embryonic lethality was also reported in *lats2*-/- mice during E10.5-E12.5, as a consequence of developmental delay, with blood-filled pericardium and haemorrhaging in the head region (McPherson et al. 2004), which further highlights role of *lats2* during embryonic development.

The distinct expression between *lats1* and *lats2* was observed in mouse embryos during early development (E8.5-E10.5) mainly in tissue of ectodermal and mesodermal origin, respectively. Elevated *lats1* expression was observed in the neural tube, neuroepithelium, head fold and auditory vesicles, mesencephalon at E8.5-10.5. At the same time, increased *lats2* mRNA was found in somites, cardiac region, and lateral mesodermal plate. However, weaker expression of *lats2* was observed in developing gut, lungs, and head mesenchyme. Interestingly, the authors found overlapping *lats1* and *lats2* expression in branchial arches at E8.5 (McPherson et al. 2004). Similarly, in mouse developing pituitary gland (10.5-17.5dpc) *lats1* maintained high expression whereas *lats2* was barely detected (Lodge et al. 2016). Considering, different experimental models, we expect variation in the expression profile. Nonetheless, more prominent expression levels of *lats1* in the embryonic mouse are in accordance with our observations.

- ***yap* and *taz***

yap displayed ubiquitous expression in the mesenchymal compartment in the three stages studied (Figure 7a-c). Conversely, the epithelial compartment was completely absent from *yap* expression (Figure 7d, asterisks). Mahoney et al. reported that *yap* transcript is ubiquitously distributed along the epithelial compartment of embryonic mouse lung (E10.5-E18.5) (Mahoney, 2014). A recent study also demonstrated increased nuclear YAP expression (at E13.5) mainly in the pulmonary epithelium. However, stomach and intestine showed upregulated YAP in the mesenchymal compartment (Cotton et al. 2017).

Furthermore, *yap* transcript was also reported in the mesenchyme in embryonic chick stomach (E6) (McKey et al. 2016). Regarding other organ systems, such as the developing murine pituitary gland, *yap* displayed interchanging expression, at different time points. From 10.5-17.5dpc *yap* mRNA was detected in both epithelial and mesenchymal compartments (Lodge et al. 2016). Despite these results being in opposition with our findings, *yap* compartment-specific expression may reflect organ and species-specific differences (mouse *vs* chick).

Unlike its partner *yap, taz* demonstrated region-specific expression throughout the stages studied (Figure 7e-g). Histological analysis confirmed *taz* expression only in the epithelium of the main bronchi (Figure 7f, black arrow, and asterisks). In the mammalian foetal lung, strong *taz* expression was detected in the lung buds at E12.5 and a clear expression in the respiratory epithelium was seen at E13.5. At E18.5, *taz* was only found in epithelial compartment of peripheral lung and no longer in the conducting airways (Park et al. 2004). The *taz* transcript observed in the mammalian model, especially in early stages of pulmonary development, is in agreement with the results obtained for the chick lung.

Overall, *in situ* hybridization revealed expression in different compartments of the developing lung: *yap* in the mesenchyme and *taz* in the epithelium. Even though both YAP and TAZ share the effector function in HIPPO pathway, our observations raise the possibility of distinct roles of YAP and TAZ in the chick embryonic lung. Neijigane et al. also assessed the expression pattern of both *yap* and *taz* in the embryonic stages of frog (*Xenopus tropicalis*). Despite that both genes (xt*yap* and xt*taz*) were widely expressed in facial connective tissues and branchial arch, some differences were detected. For instance, xt*yap* was present in otic vesicle, notochord, midbrain-hindbrain boundary, pronephros, hindgut, and tailbud. Whereas, xt*taz* was expressed in brain, presomitic mesoderm, trunk neural crest cells and migrating hypaxial myoblasts (Nejigane et al. 2011). Additionally, some studies report the greater influence of *yap* in cell spreading, glucose uptake, proliferation, and migration when compared to *taz* (Plouffe et al. 2018). Together, these results imply that YAP and TAZ may have overlapping and distinct functions throughout embryonic development and that, eventually, this scenario also occurs in the embryonic chick lung.

- ***tead1* and *tead4***

Both *tead1* and *tead4* transcripts are present in the mesenchymal compartment (dorsal-ventral region) of embryonic chick lung. A robust signal is observed around outgrowing secondary branches in *tead1* and *tead4* (Figure 8). The expression pattern of TEAD family members was examined in gastrulating mouse embryos (E6.5-E9.0). At E6.5 *tead4* was present in all germ layers, with increased expression in the extraembryonic region and proximally whereas *tead1* was absent. Other TEAD family members were

present in these stages (Sawada et al. 2005). *tead1-/-* double mutant embryos die around E11.5. On the other hand, ablation of the mouse *tead4* gene results in a preimplantation lethal phenotype (Yagi et al. 2007) whereas, for instance, ablation of *tead2* has no impact on development (Sawada et al. 2008). This data suggests that *tead* genes have distinct roles during development and may play a role also in lung development.

- ***ctgf***

ctgf (connective tissue growth factor) is one of the many downstream targets of HIPPO signalling pathway. We observed that this gene was present in all the stages studied, mainly in the distal-ventral region of pulmonary mesenchyme and weakly expressed in the epithelial compartment (Figure 9).

ctgf is described to have a constitutive expression in the cardiovascular system and transient expression in the cartilage formation. Moreover, strong expression of *ctgf* was also detected in small-diameter vessels (capillaries) surrounding the lung and other branching organs (Friedrichsen et al. 2003). These findings are in accordance with our observations of vascular-like *ctgf* expression in the embryonic chick lungs, in the stages studied (Figure 9d, dashed arrow). We did not detect *ctgf* mRNA in the epithelial compartment which is in accordance with a previous study (Friedrichsen et al. 2003). Moreover, studies using *ctgf* null mouse reported foetal lung hypoplasia by directly affecting cellular proliferation and apoptosis and indirectly by impaired thoracic expansion (Baguma-Nibasheka and Kablar 2008) further highlighting the relevance of this gene in pulmonary development.

The whole mount *in situ* hybridization revealed that all HIPPO pathway members were present throughout the three stages studies, except for *mst1* and *lats2*. Curiously, the core HIPPO pathway members were not restricted to only one compartment of the embryonic lung. Instead, we observed that *lats1*, *yap*, *tead1, tead4,* and *ctgf* are present in the mesenchymal compartment, while *mst1* and *taz* transcripts

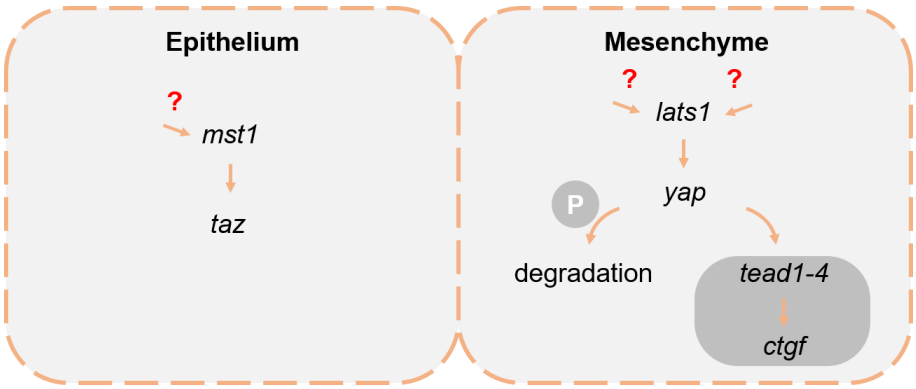

Figure 15. Schematic representation of lung compartment-specific expression of Hippo signaling members and target. The *mst1* and *taz* mRNA is present in epithelium. The *lats1, yap, tead1, tead4* and *ctgf* are expressed in mesenchymal compartment.

were found in the pulmonary epithelium (Figure 15 and Table 3). These results suggest that main HIPPO co-activators YAP and TAZ could possibly be phosphorylated through different inhibitory kinases. It is possible that in the chick lung, both proteins are contributing to different cellular responses. Nonetheless, the suspicion regarding YAP and TAZ independent regulation and different function are upon the investigation.

Despite the overlapping functions of YAP and TAZ, studies imply the opposite activity between both co-effectors, which possibly translate into different cellular responses (Sun et al. 2017). For instance, in murine myoblasts both HIPPO co-effectors contribute to myoblast proliferation. However, later in myogenesis TAZ promotes differentiation while its partner YAP enhances the undifferentiated state (Camargo et al. 2007).

While homozygous deletion of YAP results in developmental lethality at E8.5 (Morin-Kensicki et al. 2006), the TAZ knockout mice survived, yet presented cyst formation in kidneys and enlarged spaces in the lung (Hossain et al. 2007; Makita et al. 2008). Conversely, YAP overexpression induced indirect TAZ degradation in the cytoplasm whereas gain and loss of function TAZ did not affect YAP protein abundance. This phenomenon could explain apoptotic cell death when YAP is upregulated (Finch-Edmondson et al. 2015). Additionally, in the medaka fish (*Oryzias latipes*) *yap* is mandatory for tissue tension to maintain 3D body shape, while cell proliferation is dependent on taz (Porazinski et al. 2015). Indeed, both YAP and TAZ have specific domains necessary for protein-protein interaction (Plouffe et al. 2018; Liu et al. 2018) that may impact YAP/TAZ interaction with TEAD transcription factors thus shifting the gene expression profile.

Moreover, nuclear scaffold protein Parafibromin inversely regulates YAP and TAZ activity. Even though YAP binds to Parafibromin regardless of its phosphorylation status, only the tyrosine-phosphorylated form stimulated YAP function. On the other hand, TAZ appears to bind only to tyrosine-dephosphorylated Parafibromin, which promotes TAZ co-effector activity and interaction with β-catenin, which ultimately promotes the transcription of TAZ and WNT target genes (Tang et al. 2018).

5.2. Hippo signalling activity in the embryonic chick lung

The phosphorylation status of YAP/TAZ complex specifies its subcellular localization and, consequently, the outcome in terms of transcriptional activation. For instance, YAP phosphorylation by LATS may result in both cytoplasmic retention and degradation (Zhao et al. 2007; Zhao et al. 2010). On the other hand, non-phosphorylated YAP is directed to the nucleus triggering the transcription of specific genes. Both YAP

and TAZ are master regulators for a variety of cellular events, however, YAP inactivation seems to exert stronger effect when compared to TAZ. Hence, we focused on YAP phosphorylation status as an indicator of HIPPO pathway activity; protein levels of phosphorylated-YAP (pYAP) and total YAP were assessed by Western blot, in embryonic chick lungs during branching morphogenesis.

Protein expression levels of pYAP and YAP were assessed in stages b1, b2 and b3 at two time-points (0h and 48h). The western blot demonstrated similar expression levels of pYAP and YAP at basal (0h) and after 48 hours of culture (Figure 11a). As the branching morphogenesis progressed (48 hours of culture), both YAP and pYAP expression levels declined proportionally. The decrease in pYAP could be associated with a protein degradation mechanism, as reported by Zhao's team (Zhao et al. 2010), while reduction of YAP would imply the down-regulation of transcription program. Activation/inhibition of HIPPO signalling reflects in the expression profile of cells and tissues namely, in the transcription of proliferation and differentiation-related genes. The decrease in the expression levels of YAP and pYAP during chick lung organogenesis may suggest a progressive shift in the transcription of specific target genes.

To evaluate HIPPO pathway activity, we determined pYAP/YAP ratio based on the quantification of protein levels. If pYAP/YAP ratio is higher than 1 it implies that there is more cytoplasmic than nucleic YAP, hence indicating that HIPPO pathway is active; if the ratio is below 1, HIPPO pathway is off. There are minor variations in the ratio between stages and between time-points. However, the differences in pYAP/YAP ratio between Day 0 and Day 2, in three stages studied, are not statistically significant. The pYAP/YAP ratio was maintained to ≈1 reflecting similar protein levels of pYAP and YAP in the embryonic stages studied.

Similar observations were made in MCF10A cell line (non-tumorigenic epithelial cells), where the western blot analysis showed the same expression levels of both pYAP and YAP, as well as pYAP/ YAP ratio equivalent in basal conditions (Codelia et al. 2014).

Our data demonstrate regulation of YAP expression at different time-points (Day 0 and Day2) and developmental stages (b1, b2, and b3), and indicate balanced regulation between pYAP and YAP protein levels. Overall, these results revealed that the embryonic chick lung possesses the protein machinery needed to convey HIPPO pathway response during early branching stages.

5.3. Impact of Hippo signalling modulation in the embryonic chick lung

Manipulation of the HIPPO pathway *in vitro* is a straightforward method to determine its role in a tissue. HIPPO can be regulated downstream through its main effector YAP. Therefore, we selected the

pharmacological compound verteporfin (VP), which is known to interfere with YAP-TEAD complex formation thus impeding transcription of target genes, such as *ctgf*. Besides supressed YAP/TAZ-TEAD interaction, a recent study has demonstrated that VP reduces mRNA abundance of YAP and TAZ without affecting their subcellular localization (Szeto et al. 2016, 2016). Consequently, it impairs YAP/TAZ-TEAD complex interaction and further gene expression. Importantly, this downstream modulation mimics "HIPPO ON" (Figure 1).

Using *in vitro* explant culture, the embryonic lungs (stage b2) were treated with DMSO and different concentrations of VP (5, 7.5 and 10 µM), for 48 hours. DMSO was used as the control since VP was reconstituted in this solvent. We observed that lung explants cultured in 5 µM of VP supplemented media were similar to the control group (Figure 12b and e). In contrast, higher VP doses (7.5 µM and 10 µM) caused a reduction in lung size when compared to controls (Figure 12b, h and k). This effect is more evident in the highest dose tested (Figure 12b and k). Therefore, we can conclude decreased lung size in a dose-dependent manner.

In parallel, *in situ* hybridization for *ctgf*, known as HIPPO target, was performed. With this approach, we intended to validate HIPPO manipulation. Overall, we observed declined mRNA levels of *ctgf*, with increasing concentration of VP, thus confirming successful pathway activation.

Connective tissue growth factor (CTGF) is a fibroblast mitogen and angiogenic factor (Bradham et al. 1991) involved in angiogenesis, cell adhesion, cell survival, and apoptosis (Bradham et al. 1991; Babic et al. 1999; Blom et al. 2001). Moreover, *ctgf* is involved in regulation of cell cycle in human mesangial cells. *ctgf*-/- knockout mice display hypoplastic lungs due to reduced cell proliferation and increased apoptosis (Baguma-Nibasheka and Kablar 2008). The downregulation of *ctgf* transcript, as a consequence of Hippo manipulation, in the embryonic chick lungs will most certainly contribute to the reduction of lung growth (Figure 12c and l).

Subsequently, explants were analysed morphometrically and by evaluating the number of new peripheral buds formed (branching); explants cultured in 7.5 and 10 µM of VP exhibited a 15 and 40 % decreased in branching respectively (Figure 13), whereas 5 µM treated lungs are similar to control. The morphometric analysis revealed that all doses have an impact on growth. With increasing doses of VP, the effect expands from the mesenchyme (5 µM) progressively to the epithelial compartment (7.5 µM and 10 µM); ultimately, the highest dose tested displayed the most dramatic decline in all the parameters examined (Figure 14). Altogether, quantitative evaluation of lung morphology suggests that activation of HIPPO, by VP, leads to impaired lung growth by initially inducing changes in the mesenchymal

compartment; additional activation of HIPPO (with higher VP doses) impacts the epithelium causing a decrease in branching.

Aberrant branching morphogenesis was observed in *yap*$^{-null}$ murine lungs. It was found that the epithelial compartment did not respond to mesenchymal TGF-β signalling in the absence of YAP. Also, the mRNA levels of *smad7* (epithelial target of TGF-β) were downregulated (Mahoney et al. 2014). It was proposed that nuclear YAP-TEAD complexes cooperate with TGF-β induced signals to activate the lung transcriptional program. It is possible that, also in the chick lung, the inhibition of YAP-TEAD association (by VP) will compromise TGF-βsignalling thus impairing branching. For instance, in the chick developing lung, *tgfβ2* mRNA is present in the mesenchyme surrounding the secondary bronchi and may be a part of this mechanism (Fernandes-Silva et al. 2017). In the murine lung, defects in branching are also associated with lack of epithelial cells and improper force generation (Lin et al. 2017).

Recent studies highlighted the interaction between HIPPO core members and WNT signalling (Tang et al. 2018; Park et al. 2015; Imajo et al. 2012; Zhao et al. 2010). Park et al. described an alternative WNT-YAP/TAZ (Wnt-FZD/ROR-Ga12/13-Rho-Lats1/2-YAP/TAZ) signalling cascade, which antagonizes canonical WNT/βcatenin pathway. The WNT-YAP/TAZ was manipulated downstream by inhibiting YAP/TAZ-TEAD complex (using VP). The VP treatment downregulated WNT5A and CTGF expression but upregulated β-catenin/TCF target genes like *c-myc* and *sox9*. Therefore, canonical WNT/βcatenin signalling inhibition is induced through YAP/TAZ with TEAD-regulated transcriptional machinery (Park et al. 2015). WNT signalling is crucial for chick lung development (Moura et al. 2014). Several canonical and non-canonical ligands are expressed in the embryonic lung; moreover, WNT inhibition causes a decrease in branching. As it occurs in other tissues and systems, there might be a crosstalk between HIPPO and WNT/β-catenin signalling that contributes to the observed phenotype.

5.4. Toxicity assessment

The morphometric evaluation demonstrated a reduction in the overall lung size upon VP-treatment, which could imply either upregulated cell death or supressed proliferation or both. In fact, VP toxicity has been previously reported in several studies (Dasari et al. 2017; Konstantinou et al. 2017; Ammar and Kahook 2013). To examine the potential cellular damage due to VP, cytotoxicity was evaluated by measuring Lactate Dehydrogenase (LDH) activity. When an injury occurs, this cytoplasmic enzyme leaks through the impaired plasma membrane. Ultimately, the increased amount of LDH activity in the culture media could be a good indicator of tissue damage.

We did not detect increased levels of LDH activity in the culture medium, including the medium treated with 10 μM of VP. LDH is used as primary assay for screening cytotoxicity, however, some key points should be foreseen as, for instance, morphological properties and architecture of the tissues that are selected for *in vitro* culture (whole organ vs cell). The whole organ is a 3D structure composed of the extracellular matrix and multiple cell layers. In cell cultures, upon plasma membrane damage LDH enzyme is directly released into the medium. Conversely, in whole organ it may stay "trapped" in the extracellular matrix and not reach culture medium, hence resulting in impeded detection of LDH. Therefore, when complex structures are involved, controlled tissue disruption, without causing any additional damage to the plasma membrane, should be performed to measure cytotoxicity.

Moreover, the lung medium used for the *in vitro* experiments was supplemented with serum that may contain LDH. It has been suggested that media supplementation with foetal bovine serum (FBS) can interfere with assay sensitivity and obscure cellular LDH levels. In fact, cells cultured in 5-10% FBS supplemented media, after cytotoxic exposure, showed less LDH release when compared to 1% FBS (Hiebl et al. 2017). Consistent with the previous report, supplementation with 5, 10 and 15% FBS increased LDH content in a dose-dependent manner. In addition, residual LDH was detected in heat-inactivated FBS, when compared to serum-free media (Thomas et al. 2015). Another study suggests the possibility of extracellular LDH degradation when reactive chemicals such as ascorbate or glutathione (GSH) are present. The LDH from rabbit muscle in menadione and H2O2-induced toxicity was suppressed with the addition of ascorbate (1 mM), while the glutathione (GSH) caused an increase in LDH activity, hence indicating different LDH reactivity with other compounds. Nonetheless, the authors speculate that intracellular LDH could be preserved from inactivation through other reactions occurring within cell cytoplasm (Kendig and Tarloff 2007).

Overall, we cannot rule out the possibility that the reduction in lung size may be due to increased cellular damage, despite the fact that LDH activity in all conditions (5, 7.5 and 10 μM of VP) was indistinguishable to controls and suggests no cellular damage upon VP treatment. Eventually, the dramatic decrease in lung size may be due to a reduction in proliferation that could be sufficient to impair normal lung growth, without upregulating cell death.

It has been reported that VP impacts on cell proliferation. For instance, the ovarian cancer weight was dramatically reduced in OVAR8 xenografts when treated with VP (Feng et al. 2016). The excessive liver overgrowth caused by *nf2* knockout or YAP upregulation was reversed with VP-treatment (Liu-Chittenden et al. 2012). In both cases, a reduction in proliferation was described. VP also inhibited proliferation of

human PDAC (pancreatic ductal adenocarcinoma) PANC1 and SW1990 cells via arrest at G1 phase. The cell cycle associated genes, *cyclinD1* and *cyclinE1*, were downregulated in a dose-dependent manner due to impaired YAP-TEAD interaction (Wei et al. 2017). Another study suggests, that VP anti-proliferative effect operates via Caspase-3 mediated apoptosis, regardless of YAP. Moreover, the pYAP and total YAP levels were declined after VP treatment in HEC1A, HEC1B (endometrial carcinoma) cell lines, and organoids, indicating diminished YAP expression (Dasari et al. 2017).

Chen et al. also reported declined pYAP and YAP protein expression levels, which is consistent to previous findings by Ramesh-Dasari et al. Curiously, the upstream YAP inhibitory kinase LATS1 and MST1 expression was also downregulated. The proliferation was also supressed in NB4 cell line by VP treatment, via inducing G0/G1 phase cell cycle arrest and supressed CYCLIN D1 protein expression levels. Moreover, upregulated cleaved-caspase3 expression in this line was also observed, pointing to both inhibition of the proliferation and induction of apoptosis (Chen et al. 2017).

The proliferation arrest was observed in KLE and EFE184 cell lines when treated with VP, in a dose-dependent manner. Moreover, prolonged exposure (20 hours) to VP (3 μM) resulted in cell vacuolization (Wang et al. 2016). The VP localization in mitochondria possibly modulates YAP/TAZ expression through mitochondrial fusion (Gibault et al. 2017). The upregulated YKI (YAP in *Drosophila*) promotes the transcription of *opa1* and *marf* resulting in mitochondrial fusion (Nagaraj et al. 2012), which is associated with G1-S phase of cell cycle. Transient mitochondrial hyperfusion leads to CYCLIN E build-up and DNA replication. Continuous hyperfusion causes increased expression of CYCLIN E and impaired cell cycle (cells at G0 phase entering S phase) (Mitra et al. 2009). The cell cycle progression requires CYCLIN-CDK complexes. For instance, CYCLIN C-CDK3 is active at G0/G1 transition (Ren and Rollins 2004), CYCLIN D- CDK4/6 at G1, while CYCLIN E- CDK2 at G1/S phase (Musgrove 2006). The impaired regulation of cyclins, especially CYCLIN D and CYCLIN E is associated with carcinogenesis in breast (Arnold and Papanikolaou 2005; Keyomarsi et al. 2002), lung (Gautschi et al. 2007; Li et al. 2008; Santarius et al. 2010), pancreas (Garcea et al. 2005), head and neck (Thomas et al. 2005). Also, it was observed, that CYCLIN D1 is a common target of YAP and β-catenin in colon cancer (Varelas et al. 2010).

Together, the studies are consistent with VP-induced proliferative arrest in tumorigenesis mainly through the inhibition of YAP/TAZ-TEAD interaction, leading to supressed transcription of target genes. Therefore, it is likely that VP-mediated effect during embryonic development may be anti-proliferative too. Considering the results from branching (Figure 13) and morphometric (Figure 14) analysis, the decreased overall lung size could be attributed to a dramatic decline in cellular proliferation, even though we did not assess

proliferation of chick lung explants after VP treatment. Based on previous reports, proliferation is inhibited by VP in a concentration-dependent manner (Chen et al. 2017), which consistent with impaired chick lung growth in our study (Figure 12-14).

Overall our data reveals, for the first time, the presence of HIPPO signalling in early stages of avian pulmonary branching. Based on gene/protein expression profile and pathway modulation studies, we show that HIPPO is active and possibly involved in the regulation of lung growth.

6.CONCLUSIONS AND FUTURE PERSPECTIVES

HIPPO signalling is involved in numerous cellular events as, for instance, organ growth control during embryonic development and tumorigenesis. The phosphorylation status of HIPPO co-effectors YAP and TAZ impact TEAD-mediated transcription of target genes that convey the pertinent cellular responses. Additionally, HIPPO pathway inhibition exerts organ-specific phenotypic differences. Therefore, the aim of our study was to disclose the role of HIPPO in the developing respiratory system of the avian animal model.

The HIPPO cascade characterization using *in situ* hybridization revealed, that all pathway members were present in the chick lung, except for *mst2* and *lats2*, due to minor differences between mammalian and avian model. Surprisingly, the existing HIPPO members demonstrated compartment-specific expression. For instance, *mst1* and *taz* were present in the epithelial compartment whereas, *lats1*, *yap, tead1, tead4* and HIPPO target *ctgf* were expressed in mesenchymal compartment. This is not in accordance with the mammalian model, in which YAP and TAZ are both present in the epithelial compartment. Our data suggests different roles of *yap* and *taz* in the embryonic chick lung and, eventually, different signal transduction pathways (Figure 13 and Table 3). Additionally, other, yet unidentified kinase, might be involved in MST/LATS-mediated phospho-regulation of YAP/TAZ. Thus, assessing spatial distribution of *sav* and *mob1a/b* and upstream regulator *nf2* (encoded for protein Merlin), could be further approached. Moreover, the spatial distribution of YAP and pYAP could be assessed to confirm and expand our knowledge on the subcellular location of both forms.

The *in vitro* HIPPO modulation study (via inhibited YAP-TEAD interaction) revealed, that lung explants cultured in 7.5 and 10 μM of VP supplemented media exhibited a decrease in overall lung size and branching in contrast to control (Figure 9 and 10). It is worth noting, that successful HIPPO modulation with VP was confirmed by decreased mRNA levels of target gene *ctgf* (Figure 8). These changes in lung architecture, due to VP treatment, suggest upregulated cell death or suppressed proliferation. Therefore, we first assessed VP-induced toxicity in chick lung explants with LDH assay, by evaluating culture media (after 24 and 48 hours) for cytosolic LDH enzyme. Surprisingly, no toxicity was detected. To further confirm these finding, the LDH assay in tissue lysates should be performed. Additionally, TUNEL assay could be performed to assess apoptosis. Aside of elevated cell death (yet to be confirmed), the dramatic decline in proliferation could be sufficient to impair lung growth. Thus, proliferation could also be assessed either by using EdU kit or by measuring Ki67 protein levels.

Branching defects in VP-treated lung explants could be due impaired signalling of TGF-β or canonical WNT/β-catenin pathways, which could be further explored. Afterall, the expression pattern of TGF-β and

WNT/β-catenin core members are confirmed in embryonic chick lung (Cooley et al. 2014, Moura et al. 2014). Additionally, HIPPO signalling crosstalk with other pathways contributing to correct lung patterning and development such as FGF, SHH and RA, require further investigation. We propose, a detailed expression pattern analysis, by *in situ* hybridization, for of *spry2, gli1* and *meis2* (respective markers for FGF, SHH and RA) in VP-treated and control lung explant.

Our study demonstrated, for the first time in the avian animal model, that HIPPO machinery is present in embryonic lung, in the stages studied (b1, b2 and b3). Protein analysis of pYAP and YAP expression levels revealed that pathway is active during early branching morphogenesis of chick lung. Altogether, this study suggests that HIPPO is conserved between mammalian and avian models similarly to other signalling pathways. The pathway modulation experiment implies that when HIPPO is "ON" there is an impairment lung growth and branching (Figure 1a). Nonetheless, further examination on molecular mechanisms involved, would provide the insights of Hippo regulated organ growth control.

7.ANNEX I

Figure 1. *mst2* expression pattern in the chick embryo. Representative example of whole mount *in situ* hybridization of HH25 embryo. *mst2* is expressed in head and ventral region (a); front and hind limbs were absent from mesenchymal expression (b, c). Amplification a – 1.6x; b, c – 4x.

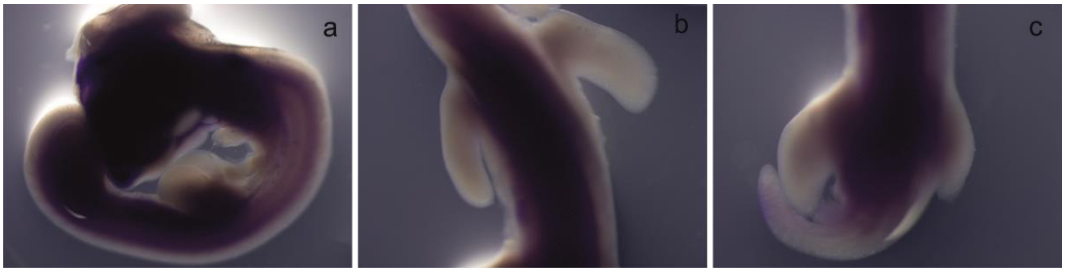

Figure 2. *lats2* expression patter in the chick embryo. Representative example of whole mount *in situ* hybridization of HH25 embryo. *lats2* has weak expression in head and ventral-distal region (a); front and hind limbs were absent from mesenchymal expression (b, c). Amplification a – 2.5x; b, c – 3.2x.

8.REFERENCES

- Abylkassov, Ramazan; Xie, Yingqiu (2016): Role of Yes-associated protein in cancer. An update. In Oncol Lett 12 (4), pp. 2277–2282.
- Adler, J. J.; Heller, L. B.; Bringman, R. L.; Ranahan, P. W.; Cocklin, R. R.; Goebl, G. M. et al. (2013): Amot130 Adapts Atrophin-1 Interacting Protein 4 to Inhibit Yes-associated Protein Signaling and Cell Growth. In J. Biol. Chem. 288 (21), pp. 15181–15193.
- Al-Moujahed, Ahmad; Brodowska, Katarzyna; Stryjewski, Tomasz P.; Efstathiou, Nikolaos E.; Vasilikos, Ioannis; Cichy, Joanna et al. (2017): Verteporfin inhibits growth of human glioma in vitro without light activation. In Sci Rep. 7 (1), p. 7602.
- Ammar, A. D.; Kahook, Y. M. (2013): In vitro effects of verteporfin on ocular cells. In Mol Vis. (19), pp. 424–429.
- Anani, Shihadeh; Bhat, Shivani; Honma-Yamanaka, Nobuko; Krawchuk, Dayana; Yamanaka, Yojiro (2014): Initiation of Hippo signalling is linked to polarity rather than to cell position in the pre-implantation mouse embryo. In Development 141 (14), pp. 2813–2824.
- Anastas, Jamie N.; Moon, Randall T. (2013): WNT signalling pathways as therapeutic targets in cancer. In Nat. Rev. Cancer 13 (1), pp. 11–26.
- Aragona, Mariaceleste; Panciera, Tito; Manfrin, Andrea; Giulitti, Stefano; Michielin, Federica; Elvassore, Nicola et al. (2013): A mechanical checkpoint controls multicellular growth through YAP/TAZ regulation by actin-processing factors. In Cell 154 (5), pp. 1047–1059.
- Arnold, Andrew; Papanikolaou, Alexandros (2005): Cyclin D1 in breast cancer pathogenesis. In J. Clin. Oncol. 23 (18), pp. 4215–4224.
- Babic, Alexander M.; Chen, Chih-Chiun; Lau, Lester F. (1999): Fisp12/Mouse Connective Tissue Growth Factor Mediates Endothelial Cell Adhesion and Migration through Integrin αv β3, Promotes Endothelial Cell Survival, and Induces Angiogenesis In Vivo. In Mol. Cell. Biol. 19 (4), pp. 2958–2966.
- Baguma-Nibasheka, Mark; Kablar, Boris (2008): Pulmonary hypoplasia in the connective tissue growth factor (Ctgf) null mouse. In Dev. Dyn. 237 (2), pp. 485–493.
- Bao, Yijun; Nakagawa, Kentaro; Yang, Zeyu; Ikeda, Mitsunobu; Withanage, Kanchanamala; Ishigami-Yuasa, Mari et al. (2011): A cell-based assay to screen stimulators of the Hippo pathway reveals the inhibitory effect of dobutamine on the YAP-dependent gene transcription. In Eur. J. Biochem. 150 (2), pp. 199–208.
- Bjørnstad, Sigrid; Austdal, Lars Peter Engeset; Roald, Borghild; Glover, Joel Clinton; Paulsen, Ragnhild Elisabeth (2015): Cracking the Egg. Potential of the Developing Chicken as a Model System for Nonclinical Safety Studies of Pharmaceuticals. In J. Pharmacol. Exp. Ther. 355 (3), pp. 386–396.
- Blom, Ingrid E.; van Dijk, Anette J.; Wieten, Lotte; Duran, Karen; Ito, Yasuhiko; Kleij, Livio et al. (2001): In vitro evidence for differential involvement of CTGF, TGFβ and PDGF-BB in mesangial response to injury. In Nephrol. Dial. Transplant. 16 (6), pp. 1139–1148.

- Boggiano, J.C.; Vanderzalm, P.J.; Fehon, R.G. (2011): Tao-1 phosphorylates Hippo/MST kinases to regulate the Hippo-Salvador-Warts tumor suppressor pathway. In Dev Cell 21(5):888-95.
- Bradham, M. D.; Igarashi, A.; Potter L. R.; Grotendorst, G. R. (1991): Connective Tissue Growth Factor : a Cysteine-rich Mitogen Secreted by Human Vascular Endothelial Cells Is Related to the SRC-induced Immediate Early Gene Product CEF10. In J Cell Biol. 114 (6), pp. 1285–1294.
- Brown, S. M.; Goldstein, L. J. (1997): The SREBP Pathway: Regulation of Cholesterol Metabolism by Proteolysis of a Membrane-Bound Transcription Factor. In Cell 89, pp. 331–340.
- Camargo, Fernando D.; Gokhale, Sumita; Johnnidis, Jonathan B.; Fu, Dongdong; Bell, George W.; Jaenisch, Rudolf; Brummelkamp, Thijn R. (2007): YAP1 increases organ size and expands undifferentiated progenitor cells. In Curr Biol 17 (23), pp. 2054–2060.
- Cao, Xinwei; Pfaff, Samuel L.; Gage, Fred H. (2008): YAP regulates neural progenitor cell number via the TEA domain transcription factor. In Genes Dev. 22 (23), pp. 3320–3334.
- Cardoso, W. V.; Williams, M. C.; Mitsialis, S. A.; Joyce-Brady, M.; Rishi, A. K.; Brody, J. S. (1995): Retinoic acid induces changes in the pattern of airway branching and alters epithelial cell differentiation in the developing lung in vitro. In Am. J. Respir. Cell Mol. Biol. 12 (5), pp. 464–476.
- Cardoso, Wellington V.; Lü, Jining (2006): Regulation of early lung morphogenesis. Questions, facts and controversies. In Development 133 (9), pp. 1611–1624.
- Cardoso, Wellington V.; Mitsialis, S. Alex; Brody, Jerome S.; Williams, Mary C. (1996a): Retinoic acid alters the expression of pattern-related genes in the developing rat lung. In Dev. Dyn. 207 (1), pp. 47–59.
- Chan, S. W.; Lim, C. J.; Guo, K.; Ng, C. P.; Lee, I.; Hunziker, W. et al. (2008): A Role for TAZ in Migration, Invasion, and Tumorigenesis of Breast Cancer Cells. In Clin. Cancer Res. 68 (8), pp. 2592–2598.
- Chen, Min; Zhong, Liang; Yao, Shi-Fei; Zhao, Yi; Liu, Lu; Li, Lian-Wen et al. (2017): Verteporfin Inhibits Cell Proliferation and Induces Apoptosis in Human Leukemia NB4 Cells without Light Activation. In Int. J. Med. Sci. 14 (10), pp. 1031–1039.
- Cockburn, Katie; Biechele, Steffen; Garner, Jodi; Rossant, Janet (2013): The Hippo pathway member Nf2 is required for inner cell mass specification. In Curr Biol 23 (13), pp. 1195–1201.
- Cockburn, Katie; Rossant, Janet (2010): Making the blastocyst. Lessons from the mouse. In J. Clin. Invest. 120 (4), pp. 995–1003.
- Codelia, Veronica A.; Sun, Gongping; Irvine, Kenneth D. (2014): Regulation of YAP by mechanical strain through Jnk and Hippo signalling. In Curr Biol 24 (17), pp. 2012–2017.
- Cooley, J.R.; Yatskievych, T.A.; Antin, P.B. (2014): Embryonic expression of the transforming growth factor beta ligand and receptor genes in chicken. In Dev Dyn. 243(3):497-508
- Cotton, Jennifer L.; Li, Qi; Ma, Lifang; Park, Joo-Seop; Wang, Jiayi; Ou, Jianhong et al. (2017): YAP/TAZ and Hedgehog Coordinate Growth and Patterning in Gastrointestinal Mesenchyme. In Dev Cell. 43 (1), pp. 35-47.e4.

- Dai, Xiaoming; Liu, Huan; Shen, Shuying; Guo, Xiaocan; Yan, Huan; Ji, Xinyan et al. (2015): YAP activates the Hippo pathway in a negative feedback loop. In Cell Res. 25 (10), pp. 1175–1178.
- Dasari, R. V.; Mazack, V.; Feng, W.; Nash, J.; Carey, J. D.; Gogoi, R. (2017): Verteporfin exhibits YAP-independent anti-proliferative and cytotoxic effects in endometrial cancer cells. In Oncotarget 8 (17), pp. 28628–28640.
- Deng, Yujie; Wu, Ailing; Li, Pikshan; Li, Gang; Qin, Ling; Song, Hai; Mak, Kinglun Kingston (2016): Yap1 Regulates Multiple Steps of Chondrocyte Differentiation during Skeletal Development and Bone Repair. In Cell Rep. 14 (9), pp. 2224–2237.
- DeRan, Michael; Yang, Jiayi; Shen, Che-Hung; Peters, Eric C.; Fitamant, Julien; Chan, Puiyee et al. (2014): Energy stress regulates hippo-YAP signaling involving AMPK-mediated regulation of angiomotin-like 1 protein. In Cell Rep. 9 (2), pp. 495–503.
- Dong, Jixin; Feldmann, Georg; Huang, Jianbin; Wu, Shian; Zhang, Nailing; Comerford, Sarah A. et al. (2007): Elucidation of a universal size-control mechanism in Drosophila and mammals. In Cell 130 (6), pp. 1120–1133.
- Dupont, S.; Morsut, L.; Aragona, M.; Enzo, E.; Giulitti, S.; Cordenonsi, M. et al. (2011): Role of YAP/TAZ in mechanotransduction. In Nature 474, 179-185.
- Feng, Juntao; Gou, Jinhai; Jia, Jia; Yi, Tao; Cui, Tao; Li, Zhengyu (2016): Verteporfin, a suppressor of YAP-TEAD complex, presents promising antitumor properties on ovarian cancer. In Onco Targets Ther 9, pp. 5371–5381.
- Feng, Xiaodong; Degese, Maria Sol; Iglesias-Bartolome, Ramiro; Vaque, Jose P.; Molinolo, Alfredo A.; Rodrigues, Murilo et al. (2014): Hippo-independent activation of YAP by the GNAQ uveal melanoma oncogene through a trio-regulated rho GTPase signaling circuitry. In Cancer cell 25 (6), pp. 831–845.
- Fernandes-Silva, Hugo; Correia-Pinto, Jorge; Moura, Rute Silva (2017a): Canonical Sonic Hedgehog Signalling in Early Lung Development. In Int. J. Dev. Biol. 5 (1).
- Fernandes-Silva, Hugo; Vaz-Cunha, Patrícia; Barbosa, Violina Baranauskaite; Silva-Gonçalves, Carla; Correia-Pinto, Jorge; Moura, Rute Silva (2017b): Retinoic acid regulates avian lung branching through a molecular network. In Cell Mol Life Sci 74 (24), pp. 4599–4619.
- Finch-Edmondson, Megan L.; Strauss, Robyn P.; Passman, Adam M.; Sudol, Marius; Yeoh, George C.; Callus, Bernard A. (2015): TAZ Protein Accumulation Is Negatively Regulated by YAP Abundance in Mammalian Cells. In J. Biol. Chem. 290 (46), pp. 27928–27938.
- Frazier, Ken; Williams, Shawn; Kothapalli, Devashish; Klapper, Helene; Grotendorst, Gary R. (1996): Stimulation of Fibroblast Cell Growth, Matrix Production, and Granulation Tissue Formation by Connective Tissue Growth Factor. In J. Invest. Dermatol. 107 (3), pp. 404–411.

- Friedrichsen, Soenke; Heuer, Heike; Christ, Stephanie; Winckler, Miryam; Brauer, Daniel; Bauer, Karl; Raivich, Gennadij (2003): CTGF expression during mouse embryonic development. In Cell Tissue Res 312 (2), pp. 175–188.
- Gao, Tao; Zhou, Dawang; Yang, Chenghua; Singh, Tarjinder; Penzo-Méndez, Alfredo; Maddipati, Ravikanth et al. (2013): Hippo signalling regulates differentiation and maintenance in the exocrine pancreas. In Gastroenterology 144 (7), 1543-53, 1553.e1.
- Garcea, G.; Neal, C. P.; Pattenden, C. J.; Steward, W. P.; Berry, D. P. (2005): Molecular prognostic markers in pancreatic cancer. A systematic review. In Eur. J. Cancer 41 (15), pp. 2213–2236.
- Gautschi, Oliver; Ratschiller, Daniel; Gugger, Mathias; Betticher, Daniel C.; Heighway, Jim (2007): Cyclin D1 in non-small cell lung cancer. A key driver of malignant transformation. In Lung Cancer 55 (1), pp. 1–14.
- George, Nicholas M.; Day, Caroline E.; Boerner, Brian P.; Johnson, Randy L.; Sarvetnick, Nora E. (2012): Hippo signalling regulates pancreas development through inactivation of Yap. In Mol Cell Biol 32 (24), pp. 5116–5128.
- Gibault, Floriane; Bailly, Fabrice; Corvaisier, Matthieu; Coevoet, Mathilde; Huet, Guillemette; Melnyk, Patricia; Cotelle, Philippe (2017): Molecular Features of the YAP Inhibitor Verteporfin. Synthesis of Hexasubstituted Dipyrrins as Potential Inhibitors of YAP/TAZ, the Downstream Effectors of the Hippo Pathway. In ChemMedChem 12 (12), pp. 954–961.
- Gise, Alexander von; Lin, Zhiqiang; Schlegelmilch, Karin; Honor, Leah B.; Pan, Gina M.; Buck, Jessica N. et al. (2012): YAP1, the nuclear target of Hippo signalling, stimulates heart growth through cardiomyocyte proliferation but not hypertrophy. In Proc Natl Acad Sci U S A 109 (7), pp. 2394–2399.
- Goss, Ashley M.; Tian, Ying; Tsukiyama, Tadasuke; Cohen, Ethan David; Zhou, Diane; Lu, Min Min et al. (2009): Wnt2/2b and beta-catenin signalling are necessary and sufficient to specify lung progenitors in the foregut. In Dev Cell 17 (2), pp. 290–298.
- Green, M.R., & Sambrook, J. (2012) Molecular Cloning. A Laboratory Manual (4th edition). New York: Spring Harbor Laboratory Press.
- Guo, Liwen; Teng, Lisong (2015): YAP/TAZ for cancer therapy. Opportunities and challenges (review). In Int J Oncol 46 (4), pp. 1444–1452.
- Hamburger, V.; Hamilton, L. H. (1951): A series of normal stages in the development of the chick embryo. In Int J Morphol 88 (1), pp. 231–272.
- Harvey, Kieran F.; Pfleger, Cathie M.; Hariharan, Iswar K. (2003): The Drosophila Mst Ortholog, hippo, Restricts Growth and Cell Proliferation and Promotes Apoptosis. In Cell 114 (4), pp. 457–467.
- Henrique, D.; Adam, J.; Myat, A.; Chitnis, A.; Lewis, J.; Ish-Horowicz, D. (1995): Expression of a Delta homologue in prospective neurons in the chick. In Nature 375, pp. 787–790.

- Herriges, Michael; Morrisey, Edward E. (2014): Lung development. Orchestrating the generation and regeneration of a complex organ. In Development 141 (3), pp. 502–513.
- Hiebl, Bernhard; Peters, Sinem; Gemeinhardt, Ole; Niehues, Stefan M.; Jung, Friedrich (2017): Impact of serum in cell culture media on in vitro lactate dehydrogenase (LDH) release determination. In JCB 3 (1), pp. 9–13.
- Hong, Wanjin; Guan, Kun-Liang (2012): The YAP and TAZ transcription co-activators. Key downstream effectors of the mammalian Hippo pathway. In Semin Cell Dev Biol 23 (7), pp. 785–793.
- Hossain, Zakir; Ali, Safiah Mohamed; Ko, Hui Ling; Xu, Jianliang; Ng, Chee Peng; Guo, Ke et al. (2007): Glomerulocystic kidney disease in mice with a targeted inactivation of Wwtr1. In Proc Natl Acad Sci U S A 104 (5), pp. 1631–1636.
- Huang, Jianbin; Wu, Shian; Barrera, Jose; Matthews, Krista; Pan, Duojia (2005): The Hippo signalling pathway coordinately regulates cell proliferation and apoptosis by inactivating Yorkie, the Drosophila Homolog of YAP. In Cell 122 (3), pp. 421–434.
- Iglesias-Bartolome, Ramiro; Torres, Daniela; Marone, Romina; Feng, Xiaodong; Martin, Daniel; Simaan, May et al. (2015): Inactivation of a Gαs-PKA tumour suppressor pathway in skin stem cells initiates basal-cell carcinogenesis. In Nat Cell Biol 17 (6), pp. 793–803.
- Imajo, Masamichi; Miyatake, Koichi; Iimura, Akira; Miyamoto, Atsumu; Nishida, Eisuke (2012): A molecular mechanism that links Hippo signalling to the inhibition of Wnt/β-catenin signalling. In EMBO J. 31 (5), pp. 1109–1122.
- Jia, J.; Zhang, W.; Wang, B.; Trinko, R.; Jiang, J. (2003): The Drosophila Ste20 family kinase dMST functions as a tumor suppressor by restricting cell proliferation and promoting apoptosis. In Genes Dev. 17, 2514–2519.
- Jiao, Shi; Wang, Huizhen; Shi, Zhubing; Dong, Aimei; Zhang, Wenjing; Song, Xiaomin et al. (2014): A peptide mimicking VGLL4 function acts as a YAP antagonist therapy against gastric cancer. In Cancer cell 25 (2), pp. 166–180.
- Johnson, H. M.; Ziomek, A. C. (1981): The Foundation of Two Distinct Cell Lineages within the Mouse Morula. In Cell 24, pp. 71–80.
- Justice, W. R.; Zilian, O.; Woods, F. D.; Noll, M.; Bryant J. P. (1995): The Drosophila tumor suppressor gene warts encodes a homolog of human myotonic dystrophy kinase and is required for the control of cell shape and proliferation. In Genes Dev. 9(5), pp. 534-546.
- Kain, Kristin H.; Miller, James W. I.; Jones-Paris, Celestial R.; Thomason, Rebecca T.; Lewis, John D.; Bader, David M. et al. (2014): The chick embryo as an expanding experimental model for cancer and cardiovascular research. In Dev. Dyn. 243 (2), pp. 216–228.

- Kanai, F.; Marignani A. P.; Sarbassova, D.; Yagi, R.; Hall, A. R.; Donowitz, M. et al. (2000): TAZ: a novel transcriptional co-activator regulated by interactions with 14-3-3 and PDZ domain proteins. In EMBO J. 19 (24), pp. 6778–6791.
- Kango-Singh, M. (2002): Shar-pei mediates cell proliferation arrest during imaginal disc growth in Drosophila. In Development 129 (24), pp. 5719–5730.
- Kendig, M. D.; Tarloff, B. J. (2007): Inactivation of lactate dehydrogenase by several chemicals: implications for in vitro toxicology studies. In Toxicol In Vitro. 21 (1), 125–132.
- Keyomarsi, K.; Tucker, S. L.; Buchholz, T. A.; Callister, M.; Ding, Y.; Hortobagyi, G. N. et al. (2002): Cyclin E and Survival in Patients with Breast Cancer. In N Engl J Med 347 (20), pp. 1566–1575.
- Kim, Hye Young; Varner, Victor D.; Nelson, Celeste M. (2013): Apical constriction initiates new bud formation during monopodial branching of the embryonic chicken lung. In Development 140 (15), pp. 3146–3155.
- Kim, Minchul; Kim, Miju; Lee, Seunghee; Kuninaka, Shinji; Saya, Hideyuki; Lee, Ho et al. (2013b): cAMP/PKA signalling reinforces the LATS-YAP pathway to fully suppress YAP in response to actin cytoskeletal changes. In EMBO J. 32 (11), pp. 1543–1555.
- Kimura, S.; Hara, Y.; Pineau, T.; Fernandez-Salguero, P.; Fox, H. C.; Ward, M. J.; Gonzalez, J. F. (1996): The T/ebp null mouse: thyroid-specific enhancer-binding protein is essential for the organogenesis of the thyroid, lung, ventral forebrain, and pituitary. In Genes Dev. (10), pp. 60–69.
- Kling, David E.; Lorenzo, Hans K.; Trbovich, Alexander M.; Kinane, T. Bernard; Donahoe, Patricia K.; Schnitzer, Jay J. (2002): MEK-1/2 inhibition reduces branching morphogenesis and causes mesenchymal cell apoptosis in fetal rat lungs. In American journal of physiology. Lung cellular and molecular physiology 282 (3), L370-8.
- Konstantinou, Eleni K.; Notomi, Shoji; Kosmidou, Cassandra; Brodowska, Katarzyna; Al-Moujahed, Ahmad; Nicolaou, Fotini et al. (2017): Verteporfin-induced formation of protein cross-linked oligomers and high molecular weight complexes is mediated by light and leads to cell toxicity. In Sci. Rep. 7, p. 46581.
- Lai, Eric C. (2004): Notch signalling. Control of cell communication and cell fate. In Development 131 (5), pp. 965–973.
- Lai, Zhi-Chun; Wei, Xiaomu; Shimizu, Takeshi; Ramos, Edward; Rohrbaugh, Margaret; Nikolaidis, Nikolas et al. (2005): Control of cell proliferation and apoptosis by mob as tumor suppressor, mats. In Cell 120 (5), pp. 675–685.
- Lange, Alexander W.; Sridharan, Anusha; Xu, Yan; Stripp, Barry R.; Perl, Anne-Karina; Whitsett, Jeffrey A. (2015): Hippo/Yap signalling controls epithelial progenitor cell proliferation and differentiation in the embryonic and adult lung. In J Mol Cell Biol 7 (1), pp. 35–47.
- Li, Peng; Chen, Ying; Mak, Kinglun Kingston; Wong, Chun Kwok; Wang, Chi Chiu; Yuan, Ping (2013): Functional role of Mst1/Mst2 in embryonic stem cell differentiation. In PloS one 8 (11), e79867.

- Li, Rong; An, She-Juan; Chen, Zhi-Hong; Zhang, Guo-Chun; Zhu, Jian-Quan; Nie, Qiang et al. (2008): Expression of cyclin D1 splice variants is differentially associated with outcome in non-small cell lung cancer patients. In Hum. Pathol. 39 (12), pp. 1792–1801.
- Li, Yina; Gordon, Julie; Manley, Nancy R.; Litingtung, Ying; Chiang, Chin (2008): Bmp4 is required for tracheal formation. A novel mouse model for tracheal agenesis. In Dev Biol 322 (1), pp. 145–155.
- Lin, C.; Yao, E.; Zhang, K.; Jiang, X.; Croll, S.; Thompson-Peer, K.; Chuang, Pao-Tien. (2017): YAP is essential for mechanical force production and epithelial cell proliferation during lung branching morphogenesis. eLife. 6, pp. e21130.
- Lin, Chuwen; Yao, Erica; Chuang, Pao-Tien (2015): A conserved MST1/2-YAP axis mediates Hippo signalling during lung growth. In Dev Biol 403 (1), pp. 101–113.
- Liu, Huirong; Du, Suya; Lei, Tiantian; Wang, Hailian; He, Xia; Tong, Rongsheng; Wang, Yi (2018): Multifaceted regulation and functions of YAP/TAZ in tumors (Review). In Oncol. Rep. 40 (1), pp. 16–28.
- Liu-Chittenden, Y.; Huang, B.; Shim, S. J.; Chen, Q.; Lee, Se-Jin; Anders, A. R. et al. (2012): Genetic and pharmacological disruption of the TEAD–YAP complex suppresses the oncogenic activity of YAP. In Genes Dev. 26, pp. 1300–1305.
- Lodge, Emily J.; Russell, John P.; Patist, Amanda L.; Francis-West, Philippa; Andoniadou, Cynthia L. (2016): Expression Analysis of the Hippo Cascade Indicates a Role in Pituitary Stem Cell Development. In Front Physiol. 7, p. 114.
- Lorda-Diez, Carlos I.; Montero, Juan A.; Diaz-Mendoza, Manuel J.; Garcia-Porrero, Juan A.; Hurle, Juan M. (2011): Defining the earliest transcriptional steps of chondrogenic progenitor specification during the formation of the digits in the embryonic limb. In PloS one 6 (9), e24546.
- Lu, Li; Li, Ying; Kim, Soo Mi; Bossuyt, Wouter; Liu, Pu; Qiu, Qiong et al. (2010): Hippo signalling is a potent in vivo growth and tumor suppressor pathway in the mammalian liver. In Proc Natl Acad Sci U S A 107 (4), pp. 1437–1442.
- Mahoney, John E.; Mori, Munemasa; Szymaniak, Aleksander D.; Varelas, Xaralabos; Cardoso, Wellington V. (2014): The hippo pathway effector Yap controls patterning and differentiation of airway epithelial progenitors. In Dev Cell 30 (2), pp. 137–150.
- Makita, Ryosuke; Uchijima, Yasunobu; Nishiyama, Koichi; Amano, Tomokazu; Chen, Qin; Takeuchi, Takumi et al. (2008): Multiple renal cysts, urinary concentration defects, and pulmonary emphysematous changes in mice lacking TAZ. In Am. J. Physiol. Renal Physiol. 294 (3), F542-53.
- McKey, Jennifer; Martire, Delphine; Santa Barbara, Pascal de; Faure, Sandrine (2016): LIX1 regulates YAP1 activity and controls the proliferation and differentiation of stomach mesenchymal progenitors. In BMC Biol 14, p. 34.

- McPherson, John Peter; Tamblyn, Laura; Elia, Andrew; Migon, Eva; Shehabeldin, Amro; Matysiak-Zablocki, Elzbieta et al. (2004): Lats2/Kpm is required for embryonic development, proliferation control and genomic integrity. In EMBO J. 23 (18), pp. 3677–3688.
- Meng, Zhipeng; Moroishi, Toshiro; Guan, Kun-Liang (2016): Mechanisms of Hippo pathway regulation. In Genes Dev. 30 (1), pp. 1–17.
- Metzger, Ross J.; Klein, Ophir D.; Martin, Gail R.; Krasnow, Mark A. (2008): The branching programme of mouse lung development. In Nature 453 (7196), pp. 745–750.
- Miller, Eric; Yang, Jiayi; DeRan, Michael; Wu, Chunlei; Su, Andrew I.; Bonamy, Ghislain M. C. et al. (2012): Identification of serum-derived sphingosine-1-phosphate as a small molecule regulator of YAP. In Chem. Biol. 19 (8), pp. 955–962.
- Minoo, P.; Su, G.; Drum, H.; Bringas, P.; Kimura, S. (1999): Defects in tracheoesophageal and lung morphogenesis in Nkx2.1(-/-) mouse embryos. In Dev Biol 209 (1), pp. 60–71.
- Mitra, Kasturi; Wunder, Christian; Roysam, Badrinath; Lin, Gang; Lippincott-Schwartz, Jennifer (2009): A hyperfused mitochondrial state achieved at G1-S regulates cyclin E buildup and entry into S phase. In Proc Natl Acad Sci U S A 106 (29), pp. 11960–11965.
- Mo, Jung-Soon; Meng, Zhipeng; Kim, Young Chul; Park, Hyun Woo; Hansen, Carsten Gram; Kim, Soohyun et al. (2015): Cellular energy stress induces AMPK-mediated regulation of YAP and the Hippo pathway. In Nat Cell Biol 17 (4), pp. 500–510.
- Morikawa, Yuka; Zhang, Min; Heallen, Todd; Leach, John; Tao, Ge; Xiao, Yang et al. (2015): Actin cytoskeletal remodeling with protrusion formation is essential for heart regeneration in Hippo-deficient mice. In Sci Signal 8 (375), ra41.
- Morin-Kensicki, Elizabeth M.; Boone, Brian N.; Howell, Michael; Stonebraker, Jaclyn R.; Teed, Jeremy; Alb, James G. et al. (2006): Defects in yolk sac vasculogenesis, chorioallantoic fusion, and embryonic axis elongation in mice with targeted disruption of Yap65. In Mol Cell Biol 26 (1), pp. 77–87.
- Moroishi, T.; Park, W. H.; Qin, B.; Chen, Q.; Meng, Z.; Plouffe, W. S. et al. (2015): A YAP/TAZ-induced feedback mechanism regulates Hippo pathway homeostasis. In Genes Dev. 29, pp. 1271–1284.
- Morrisey, Edward E.; Hogan, Brigid L. M. (2010): Preparing for the first breath. Genetic and cellular mechanisms in lung development. In Dev Cell 18 (1), pp. 8–23.
- Moura, Rute S.; Coutinho-Borges, José P.; Pacheco, Ana P.; Damota, Paulo O.; Correia-Pinto, Jorge (2011): FGF signalling pathway in the developing chick lung. Expression and inhibition studies. In PloS one 6 (3), e17660.
- Moura, Rute Silva; Carvalho-Correia, Eduarda; daMota, Paulo; Correia-Pinto, Jorge (2014): Canonical Wnt signalling activity in early stages of chick lung development. In PloS one 9 (12), e112388.

- Moura, Rute Silva; Silva-Gonçalves, Carla; Vaz-Cunha, Patrícia; Correia-Pinto, Jorge (2016): Expression analysis of Shh signaling members in early stages of chick lung development. In Histochem Cell Biol 146 (4), pp. 457–466.
- Moya, Iván M.; Halder, Georg (2016): The Hippo pathway in cellular reprogramming and regeneration of different organs. In Curr. Opin. Cell Biol. 43, pp. 62–68.
- Moya, Iván M.; Halder, Georg (2016): The Hippo pathway in cellular reprogramming and regeneration of different organs. In Curr. Opin. Cell Biol. 43, pp. 62–68.
- Musgrove, Elizabeth A. (2006): Cyclins: Roles in mitogenic signaling and oncogenic transformation. In Growth Factors 24 (1), pp. 13–19.
- Nagaraj, Raghavendra; Gururaja-Rao, Shubha; Jones, Kevin T.; Slattery, Matthew; Negre, Nicolas; Braas, Daniel et al. (2012): Control of mitochondrial structure and function by the Yorkie/YAP oncogenic pathway. In Genes Dev. 26 (18), pp. 2027–2037.
- Nejigane, Susumu; Haramoto, Yoshikazu; Okuno, Makoto; Takahashi, Shuji; Asashima, Makoto (2011): The transcriptional coactivators Yap and TAZ are expressed during early Xenopus development. In Int. J. Dev. Biol. 55 (1), pp. 121–126.
- Nishioka, Noriyuki; Inoue, Ken-Ichi; Adachi, Kenjiro; Kiyonari, Hiroshi; Ota, Mitsunori; Ralston, Amy et al. (2009): The Hippo signalling pathway components Lats and Yap pattern Tead4 activity to distinguish mouse trophectoderm from inner cell mass. In Dev Cell 16 (3), pp. 398–410.
- Nishioka, Noriyuki; Yamamoto, Shinji; Kiyonari, Hiroshi; Sato, Hiroko; Sawada, Atsushi; Ota, Mitsunori et al. (2008): Tead4 is required for specification of trophectoderm in pre-implantation mouse embryos. In Mech Dev 125 (3-4), pp. 270–283.
- Oh, Sangphil; Lee, Dongjun; Kim, Tackhoon; Kim, Tae-Shin; Oh, Hyun Jung; Hwang, Chae Young et al. (2009): Crucial role for Mst1 and Mst2 kinases in early embryonic development of the mouse. In Mol Cell Biol 29 (23), pp. 6309–6320.
- Ornitz, David M.; Yin, Yongjun (2012): Signalling networks regulating development of the lower respiratory tract. In Cold Spring Harb Perspect Biol 4 (5).
- Pantalacci, Sophie; Tapon, Nicolas; Léopold, Pierre (2003): The Salvador partner Hippo promotes apoptosis and cell-cycle exit in Drosophila. In Nat Cell Biol. 5 (10), pp. 921–927.
- Paramasivama, M.; Sarkeshikb, A.; Yates, R, J.; Fernandes, G. J. M.; McCollum, D. (2011): Angiomotin family proteins are novel activators of the LATS2 kinase tumor suppressor. In Mol Biol Cell 22, pp. 3725–3733.
- Park, Hyun Woo; Kim, Young Chul; Yu, Bo; Moroishi, Toshiro; Mo, Jung-Soon; Plouffe, Steven W. et al. (2015): Alternative Wnt Signaling Activates YAP/TAZ. In Cell 162 (4), pp. 780–794.
- Patel, Sachin H.; Camargo, Fernando D.; Yimlamai, Dean (2017): Hippo Signalling in the Liver Regulates Organ Size, Cell Fate, and Carcinogenesis. In Gastroenterology 152 (3), pp. 533–545.

- Plouffe, Steven W.; Lin, Kimberly C.; Moore, Jerrell L.; Tan, Frederick E.; Ma, Shenghong; Ye, Zhen et al. (2018): The Hippo pathway effector proteins YAP and TAZ have both distinct and overlapping functions in the cell. In J. Biol. Chem. 293 (28), pp. 11230–11240.
- Porazinski, Sean; Wang, Huijia; Asaoka, Yoichi; Behrndt, Martin; Miyamoto, Tatsuo; Morita, Hitoshi et al. (2015): YAP is essential for tissue tension to ensure vertebrate 3D body shape. In Nature 521 (7551), pp. 217–221.
- Reginensi, Antoine; Enderle, Leonie; Gregorieff, Alex; Johnson, Randy L.; Wrana, Jeffrey L.; McNeill, Helen (2016): A critical role for NF2 and the Hippo pathway in branching morphogenesis. In Nat. Commun. 7, p. 12309.
- Ren, S.; Rollins, J. B. (2004): Cyclin C/Cdk3 Promotes Rb-Dependent G0 Exit. In Cell 117 (239–251).
- Saito, Akira; Nagase, Takahide (2015): Hippo and TGF-βinterplay in the lung field. In Am J Physiol Lung Cell Mol Physiol. 309 (8), L756-67
- Sakiyama, J.; Yamagishi, A.; Kuroiwa, A. (2002): Tbx4-Fgf10 system controls lung bud formation during chicken embryonic development. In Development 130, pp. 1225–1234.
- Sakiyama, Jun-ichi; Yokouchi, Y.; Kuroiwa, A. (2000): Coordinated Expression of Hoxb Genes and Signaling Molecules during Development of the Chick Respiratory Tract. In Dev. Biol. (227), pp. 12–27.
- Santarius, Thomas; Shipley, Janet; Brewer, Daniel; Stratton, Michael R.; Cooper, Colin S. (2010): A census of amplified and overexpressed human cancer genes. In Nat. Rev. Cancer 10 (1), pp. 59–64.
- Sasaki, Hiroshi (2015): Position- and polarity-dependent Hippo signalling regulates cell fates in preimplantation mouse embryos. In Semin Cell Dev Biol 47-48, pp. 80–87.
- Sasaki, Hiroshi (2017): Roles and regulations of Hippo signalling during preimplantation mouse development. In Dev Growth Differ 59 (1), pp. 12–20.
- Sawada, Atsushi; Kiyonari, Hiroshi; Ukita, Kanako; Nishioka, Noriyuki; Imuta, Yu; Sasaki, Hiroshi (2008): Redundant roles of Tead1 and Tead2 in notochord development and the regulation of cell proliferation and survival. In Mol. Biol. Cell 28 (10), pp. 3177–3189.
- Sawada, Atsushi; Nishizaki, Yuriko; Sato, Hiroko; Yada, Yukari; Nakayama, Rika; Yamamoto, Shinji et al. (2005): Tead proteins activate the Foxa2 enhancer in the node in cooperation with a second factor. In Development 132 (21), pp. 4719–4729.
- Scheel, Hartmut; Hofmann, Kay (2003): A novel inter action motif, SARAH, connects three classes of tumor suppressor. In Curr Biol 13 (23), R899-R900.
- Singh, Anamika; Ramesh, Sindhu; Cibi, Dasan Mary; Yun, Lim Sze; Li, Jun; Li, Li et al. (2016): Hippo Signalling Mediators Yap and Taz Are Required in the Epicardium for Coronary Vasculature Development. In Cell Rep. 15 (7), pp. 1384–1393.

- Sorrentino, Giovanni; Ruggeri, Naomi; Specchia, Valeria; Cordenonsi, Michelangelo; Mano, Miguel; Dupont, Sirio et al. (2014): Metabolic control of YAP and TAZ by the mevalonate pathway. In Nat Cell Biol 16 (4), pp. 357–366.
- Steinhardt, Angela A.; Gayyed, Mariana F.; Klein, Alison P.; Dong, Jixin; Maitra, Anirban; Pan, Duojia et al. (2008): Expression of Yes-associated protein in common solid tumors. In Hum. Pathol. 39 (11), pp. 1582–1589.
- Sun, Congshan; Mello, Vanessa de; Mohamed, Abdalla; Ortuste Quiroga, Huascar P.; Garcia-Munoz, Amaya; Al Bloshi, Abdullah et al. (2017): Common and Distinctive Functions of the Hippo Effectors Taz and Yap in Skeletal Muscle Stem Cell Function. In Stem Cells Int 35 (8), pp. 1958–1972.
- Swarr, Daniel T.; Morrisey, Edward E. (2015): Lung endoderm morphogenesis. Gasping for form and function. In Annu. Rev. Cell Dev. Biol. 31, pp. 553–573.
- Szeto, Stephen G.; Narimatsu, Masahiro; Lu, Mingliang; He, Xiaolin; Sidiqi, Ahmad M.; Tolosa, Monica F. et al. (2016): YAP/TAZ Are Mechanoregulators of TGF-βSmad Signaling and Renal Fibrogenesis. In J. Am. Soc. Nephrol. 27 (10), pp. 3117–3128.
- Szymaniak, Aleksander D.; Mahoney, John E.; Cardoso, Wellington V.; Varelas, Xaralabos (2015): Crumbs3-Mediated Polarity Directs Airway Epithelial Cell Fate through the Hippo Pathway Effector Yap. In Dev Cell 34 (3), pp. 283–296.
- Taderera, J. V. (1967): Control of Lung Differentiation in Vitro. In Dev. Biol. 16 (5), pp. 489-512.
- Tang, Chao; Takahashi-Kanemitsu, Atsushi; Kikuchi, Ippei; Ben, Chi; Hatakeyama, Masanori (2018): Transcriptional Co-activator Functions of YAP and TAZ Are Inversely Regulated by Tyrosine Phosphorylation Status of Parafibromin. In iScience 2, p. 103.
- Tapon, N.; Harvey, F. K.; Bell, W. D.; Wahrer, C. R. D.; Schiripo, A. T.; Haber, A. D.; Hariharan, K. I. (2002): salvador Promotes Both Cell Cycle Exit and Apoptosis in Drosophila and Is Mutated in Human Cancer Cell Lines. In Cell 110, pp. 467–478.
- Thomas, Martin G.; Marwood, Roxanne M.; Parsons, Anna E.; Parsons, Richard B. (2015): The effect of foetal bovine serum supplementation upon the lactate dehydrogenase cytotoxicity assay. Important considerations for in vitro toxicity analysis. In Toxicol In Vitro. 30 (1 Pt B), pp. 300–308.
- Tzou, Daniel; W Spurlin, James; Pavlovich, Amira L.; Stewart, Carolyn R.; Gleghorn, Jason P.; Nelson, Celeste M. (2016): Morphogenesis and morphometric scaling of lung airway development follows phylogeny in chicken, quail, and duck embryos. In EvoDevo 7, p. 12.
- Varelas, Xaralabos; Miller, Bryan W.; Sopko, Richelle; Song, Siyuan; Gregorieff, Alex; Fellouse, Frederic A. et al. (2010): The Hippo pathway regulates Wnt/beta-catenin signaling. In Dev Cell. 18 (4), pp. 579–591.
- Vergara, M. Natalia; Canto-Soler, M. Valeria (2012): Rediscovering the chick embryo as a model to study retinal development. In Neural Dev. 7, p. 22.

- Wahab, N. A. (2002): Connective Tissue Growth Factor and Regulation of the Mesangial Cell Cycle. Role in Cellular Hypertrophy. In J. Am. Soc. Nephrol. 13 (10), pp. 2437–2445.
- Wang, C.; Zhu, X.; Feng, W.; Yu, Y.; Jeong. K.; Guo. W. et al. (2016): Verteporfin inhibits YAP function through up-regulating 14-3-3σsequestering YAP in the cytoplasm. In Am J Cancer Res 6 (1), pp. 27–37.
- Wang, Yu; Yu, Aijuan; Yu, Fa-Xing (2017): The Hippo pathway in tissue homeostasis and regeneration. In Protein Cell 8 (5), pp. 349–359.
- Warburton, David; Bellusci, Saverio; Langhe, Stijn de; Del Moral, Pierre-Marie; Fleury, Vincent; Mailleux, Arnaud et al. (2005): Molecular mechanisms of early lung specification and branching morphogenesis. In Pediatr. Res. 57 (5 Pt 2), 26R-37R.
- Wei, Honglong; Wang, Fuhai; Wang, Yong; Li, Tao; Xiu, Peng; Zhong, Jingtao et al. (2017): Verteporfin suppresses cell survival, angiogenesis and vasculogenic mimicry of pancreatic ductal adenocarcinoma via disrupting the YAP-TEAD complex. In Cancer Sci J. 108 (3), pp. 478–487.
- Woodard, Gavitt A.; Yang, Yi-Lin; You, Liang; Jablons, David M. (2017): Drug development against the hippo pathway in mesothelioma. In Transl Lung Cancer Res 6 (3), pp. 335–342
- Xiao, Guang-Hui; Chernoff, J.; Testa, R. J. (2003): NF2: The wizardry of merlin. In Genes Chromosomes Cancer 38, pp. 389–399.
- Xin, Mei; Kim, Yuri; Sutherland, Lillian B.; Murakami, Masao; Qi, Xiaoxia; McAnally, John et al. (2013): Hippo pathway effector Yap promotes cardiac regeneration. In Proc. Natl. Acad. Sci. U.S.A. 110 (34), pp. 13839–13844.
- Xu, T.; Wang, W.; Zhang, S.; Stewart, S. R.; Yu, W. (1995): Identifying tumor suppressors in genetic mosaics: the Drosophila lats gene encodes a putative protein kinase. In Development 121, pp. 1053–1063.
- Yagi, Rieko; Kohn, Matthew J.; Karavanova, Irina; Kaneko, Kotaro J.; Vullhorst, Detlef; DePamphilis, Melvin L.; Buonanno, Andres (2007): Transcription factor TEAD4 specifies the trophectoderm lineage at the beginning of mammalian development. In Development 134 (21), pp. 3827–3836.
- Yeung, Benjamin; Yu, Jihang; Yang, Xiaolong (2016): Roles of the Hippo pathway in lung development and tumorigenesis. In Int J Cancer 138 (3), pp. 533–539.
- Yin, Feng; Yu, Jianzhong; Zheng, Yonggang; Chen, Qian; Zhang, Nailing; Pan, Duojia (2013): Spatial organization of Hippo signaling at the plasma membrane mediated by the tumor suppressor Merlin/NF2. In Cell 154 (6), pp. 1342–1355.
- Yu, Fa-Xing; Luo, Jing; Mo, Jung-Soon; Liu, Guangbo; Kim, Young Chul; Meng, Zhipeng et al. (2014): Mutant Gq/11 promote uveal melanoma tumorigenesis by activating YAP. In Cancer cell 25 (6), pp. 822–830.
- Yu, Fa-Xing; Meng, Zhipeng; Plouffe, Steven W.; Guan, Kun-Liang (2015a): Hippo pathway regulation of gastrointestinal tissues. In Annu. Rev. Physiol. 77, pp. 201–227.

- Yu, Fa-Xing; Zhang, Y.; Park, W. H.; Jewell, L. J.; Chen, Q.; Deng, Y. et al. (2013): Protein kinase A activates the Hippo pathway to modulate cell proliferation and differentiation. In Genes Dev. 27, pp. 1223–1232.
- Yu, Fa-Xing; Zhao, Bin; Guan, Kun-Liang (2015): Hippo Pathway in Organ Size Control, Tissue Homeostasis, and Cancer. In Cell 163 (4), pp. 811–828.
- Yu, Fa-Xing; Zhao, Bin; Panupinthu, Nattapon; Jewell, Jenna L.; Lian, Ian; Wang, Lloyd H. et al. (2012): Regulation of the Hippo-YAP pathway by G-protein-coupled receptor signaling. In Cell 150 (4), pp. 780–791.
- Zhang, Heng; Wu, Shengnan; Xing, Da (2012): Inhibition of Aβ(25-35)-induced cell apoptosis by low-power-laser-irradiation (LPLI) through promoting Akt-dependent YAP cytoplasmic translocation. In Cell. Signal. 24 (1), pp. 224–232.
- Zhang, Nailing; Bai, Haibo; David, Karen K.; Dong, Jixin; Zheng, Yonggang; Cai, Jing et al. (2010): The Merlin/NF2 tumor suppressor functions through the YAP oncoprotein to regulate tissue homeostasis in mammals. In Dev Cell. 19 (1), pp. 27–38.
- Zhao, B.; Ye, X.; Yu, J.; Li, L.; Li, W.; Li, S. et al. (2008): TEAD mediates YAP-dependent gene induction and growth control. In Genes Dev. 22, pp. 1962–1971.
- Zhao, Bin; Li, Li; Tumaneng, Karen; Wang, Cun-Yu; Guan, Kun-Liang (2010): A coordinated phosphorylation by Lats and CK1 regulates YAP stability through SCF(beta-TRCP). In Gen Dev 24 (1), pp. 72–85.
- Zhao, Bin; Wei, Xiaomu; Li, Weiquan; Udan, Ryan S.; Yang, Qian; Kim, Joungmok et al. (2007): Inactivation of YAP oncoprotein by the Hippo pathway is involved in cell contact inhibition and tissue growth control. Gen Dev 21 (21), pp. 2747–2761
- Zhao, Rui; Fallon, Timothy R.; Saladi, Srinivas Vinod; Pardo-Saganta, Ana; Villoria, Jorge; Mou, Hongmei et al. (2014): Yap tunes airway epithelial size and architecture by regulating the identity, maintenance, and self-renewal of stem cells. Dev Cell 30 (2), pp. 151–165.
- Zhao, Rui; Fallon, Timothy R.; Saladi, Srinivas Vinod; Pardo-Saganta, Ana; Villoria, Jorge; Mou, Hongmei et al. (2014b): Yap tunes airway epithelial size and architecture by regulating the identity, maintenance, and self-renewal of stem cells. In Dev Cell 30 (2), pp. 151–165.
- Zhou, X.; Wang, S.; Wang, Z.; Feng, X.; Liu, P.; Lv, Xian-Bo et al. (2015): Estrogen regulates Hippo signaling via GPER in breast cancer. In J Clin Invest. 125 (5), pp. 2123–2135.